

1 **We would like to thanks the reviewers for their time and constructive**
2 **comments. Below we have copied the reviewer comments in plain text and**
3 **included our responses in bold text.**
4

5 Anonymous Referee #1 Received and published: 10 March 2015

6 This paper uses aircraft observations from SENEX and SEAC4RS to investigate what
7 fraction of aerosol mass and extinction in the transition layer over the southeastern U.S.
8 can be attributed to mixing vs. production. It represents a clear and careful analysis of a
9 very nice dataset. However I was disappointed that the study didn't really go the extra
10 step to connect to the big picture question of aerosol sources and seasonality in the
11 southeastern U.S. which served as motivation for the study (i.e. Goldstein et al.). The
12 results beg several questions: (1) how representative was the summer of 2013? Are these
13 results generalizable for the southeast? (2) what is the impact of this highly selective
14 analysis (sub-micron only, afternoon only, no biomass burning, no in-cloud) and how
15 does this relate to average observed aerosol extinction in the region? The AERONET
16 observation of Figure 13 suggest that the sampling may bias this dataset to low AOD,
17 limiting it relevance to mean conditions. While these airborne campaigns provide a
18 limited snapshot (which nevertheless should be mined further to identify the biases
19 associated with the sub-sampling used here), there are longer term ground and satellite
20 observations which should have been used to provide a wider context. Without such work
21 to contextualize the results, the conclusions (line 3150 lines 17 onwards) are overstated.
22

23 **The reviewer has raised several important points which we respond to in**
24 **order:**

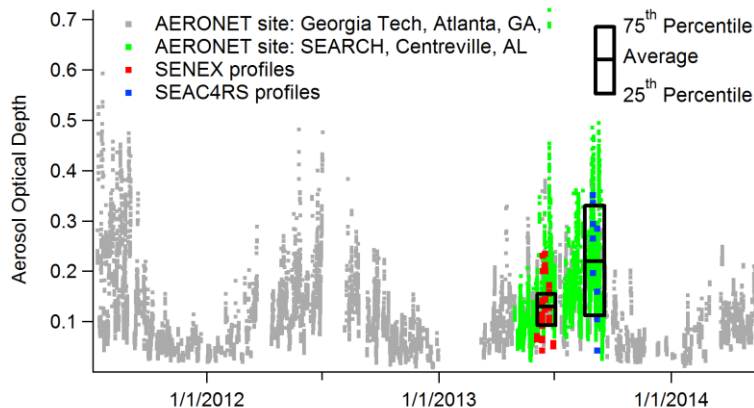
25 **1) We agree with the reviewer that adding some additional comparison with**
26 **other AOD datasets would give the conclusions more context; however, we**
27 **also would like to limit the scope of this manuscript to focus on the in situ**
28 **aerosol profiles. To that end, we have added a figure and description in the**
29 **text comparing AOD from the in situ profiles to AOD measured by**
30 **AERONET sun photometers at two locations in the SEUS. Both the figure**
31 **and additional description in the text are copied below.**
32

33 **2) The focused analysis employed here is necessary to 'resolve' the small**
34 **enhancement in the transition layer. A larger enhancement (one that would**
35 **significantly increase AOD) would be clearly apparent in the profile of**
36 **extinction (Fig. 3a). In the case of a large enhancement aloft, the extinction**
37 **would increase with altitude. Because the extinction decreases with altitude,**
38 **an analysis limited to profiles during well-developed shallow cumulus**
39 **convection was needed to resolve the smaller enhancement.**
40

41 **3) Our conclusions about the hypothesized layer of aloft are based only on**
42 **observations we made during research flights during the summer of 2013.**
43 **However, our conclusions suggest that further study of the seasonality of**
44 **AOD, meteorology affecting AOD are needed, and that the hypothesis of an**
45 **aerosol layer aloft should be re-examined. To provide more context for these**

1 conclusions we have added references (Alston et al. (2012) and Kim et al.
2 (2015)) that discuss the hypothesis of an aerosol aloft over the SEUS.

3
4 “The altitude-normalized aggregate profiles used in this analysis are drawn
5 from 37 vertical profiles; however, they represent only eight afternoons
6 during the summer of 2013. For comparison and context, Fig. 14 shows an
7 extended time series of 532 nm AOD (level 2 data) measured by AERONET
8 sun photometers [Holben et al., 2001] at the Centreville SEARCH site and at
9 the Georgia Tech site in Atlanta, Georgia. The Georgia Tech site is in an
10 urban area and is perhaps biased toward larger AOD from urban emissions,
11 while the Centreville site is rural. The sun photometers only report data
12 during cloud-free conditions. Plotted on top of these data from the sun
13 photometers are the AOD from the profiles used in the altitude-normalized
14 aggregate. These data are grouped into the profiles from the SENEX and
15 SEAC4RS studies. Aircraft profiles during the SENEX study did not sample
16 AOD greater than 0.3 while the maximum of AOD observed by the sun
17 photometers was greater than 0.4. Profiles during the SEAC4RS study,
18 although limited in number, cover a range of AOD similar to the sun
19 photometers. Because the majority of the profiles in the altitude-normalized
20 aggregate are from the SENEX study, the aggregate may be biased toward
21 cleaner conditions. The range of AOD observed during summers of 2011-
22 2013 at the Georgia Tech site indicate that the summer of 2013 is not an
23 outlier with AOD higher or lower than typical summers. This is consistent
24 with the analysis of Kim et al. [2015] who has compared satellite
25 measurements of AOD during the summers 2006-2013.”
26



27
28 **Figure 14: The AOD measured by an AERONET sun photometer in**
29 **Atlanta, GA (gray) and Centreville, AL (green). AOD from the SENEX (red)**
30 **and SEAC⁴RS (blue) profiles included in the altitude-normalized aggregate.**

1 **The black boxes show the average, 25th, and 75th percentiles of AOD from**
2 **both the SENEX and SEAC⁴RS profiles.**

3
4 1. Abstract: should state year of observations as well as campaign names

5
6 **We have added a sentence to the abstract stating the year and campaign**
7 **names.**

8
9 2. Page 3129, line 20; page 3130 line 17; page 3150, line 17: Goldstein et al., 2009 linked
10 the seasonality of AOD to biogenic SOA. Ford and Heald concludes only that the
11 observations support a significant summertime aerosol source aloft. They speculate that
12 aqueous sources of SOA or H₂SO₄ from Criegee chemistry are possible sources, so it's
13 erroneous to suggest that SOA was the hypothesis of this study.

14
15 **We thank the reviewer for pointing out the lack of nuance in our description**
16 **of the conclusions of Ford and Heald (2013). To correct this we have**
17 **rewritten sections of the abstract, introduction, and conclusion to make it**
18 **clear that the Goldstein et al. hypothesize a layer of SOA while Ford and**
19 **Heald hypothesize an aerosol layer that would be composed of organics**
20 **and/or particulate sulfate.**

21
22 3. Sections 2.1 & 2.2: Please indicate the collection efficiency of the AMS instruments
23 used and how these two instruments differ on the two aircraft.

24
25 **We have added the following text to Section 2.1.**

26
27 **“The non-refractory aerosol composition was measured by a compact time-**
28 **of-flight aerosol mass spectrometer (AMS) downstream of a pressure**
29 **controlled inlet [Bahreini et al., 2008] and most (97%) of the submicron**
30 **volume measured by the aerosol sizing instruments was transmitted into the**
31 **AMS during SENEX. The collection efficiency for the AMS was determined**
32 **by the composition for each data point using the algorithm described by**
33 **Middlebrook et al. [2012]. When comparing the volume derived from**
34 **composition (AMS plus black carbon mass) to the volume measured by the**
35 **aerosol sizing instruments in the manner outlined by Bahreini et al. [2009],**
36 **87% of the aerosol composition and sizing data from the entire SENEX study**
37 **are within the combined uncertainties.”**

38
39 **We have added the following text to Section 2.2.**

40
41 **“The non-refractory aerosol composition was measured by a high resolution**
42 **time-of-flight AMS similar to the compact time-of-flight AMS used during**
43 **the SENEX study. The two instrument differed in the resolution of the mass**
44 **spectrometer. The higher resolution AMS used during SEAC⁴RS was**
45 **operated with a 1 s sample interval. This AMS was operated similar to**
46 **Dunlea et al. [2009] and also used a pressure-controlled inlet [Bahreini et al.,**

1 **2008]. The composition-dependent formulation of Middlebrook et al. [2012]**
2 **was used to estimate the collection efficiency. The AMS sampled aerosol**
3 **downstream of a HIMIL inlet.**
4 **(<http://www.eol.ucar.edu/homes/dcrogers/Instruments/Inlets/>). In both the**
5 **HIMIL inlet and the shrouded diffuser inlet, the sampled aerosol was**
6 **initially dried by ram heating and then further dried in each instrument.”**
7

8 4. Page 3134, lines 1-5: state what wavelengths were used for the extinction
9 measurements (here or in table)

10
11 **We have add sentences to the text stating the wavelength used for the**
12 **extinction measurements.**

13 **“The extinction of dry aerosol was measured at three wavelengths (405 nm,**
14 **532 nm, and 662 nm), and humidified extinction was measured at 532 nm.**
15 **Only 532 nm extinction measurements are used in this analysis.”**
16

17 5. Table 1 and 2: aerosol extinction is listed as “dry” although the text indicates
18 measurements were taken at 3 RH conditions. Perhaps “dry” is meant to indicate the
19 uncertainty under “dry” conditions? If so, uncertainties for “wet” should also be stated.
20

21 **“Dry” was intended to indicate that the accuracy was for dry conditions. We**
22 **have added a line to Tables 1 and 2 stating the accuracy of the extinction**
23 **measurements at 90% RH. The additional uncertainty at elevated RH is due**
24 **to uncertainty in the RH measurement (+/-1%) which is translated into an**
25 **uncertainty in extinction using the kappa parameterization ($\kappa = 0.15$ typical**
26 **see Fig. 3c) and added directly, because these are likely systematic (opposed**
27 **to random) uncertainties.**
28

29 6. Table 1 and 2: Please harmonize instrument labeling: some are given in full (e.g.
30 Aerosol Mass Spectrometer) and some are given as acronyms (e.g. PTR-MS)
31

32 **We have changed the acronyms in the table to full names.**
33

34 7. Table 1 and 2: 5th entry should read “Dew Point (RH)” since the accuracy is given in
35 units of dew point, not RH.
36

37 **We have changed the 5th entry to ‘Dew point (RH)’ as suggested by the**
38 **reviewer.**
39

40 8. Section 2.4: would have been insightful for the authors to compare their extinction or
41 total AOD values to other available datasets (CALIPSO, MODIS, or AERONET).
42

43 **As suggest by the reviewer, we have added a comparison to AERONET AOD**
44 **at two sites in the SEUS. Please see our response to the overview comments of**
45 **the first reviewer above.**
46

1 9. Section 2.4: Did the authors check if the fitted kappa is consistent with the measured
2 composition?

3
4 **Another manuscript, Brock et al. (in preparation), looks at the aerosol**
5 **hygroscopicity during SENEX and SEAC⁴RS in more detail and has found**
6 **that the volume-weighted kappa from calculated from the aerosol**
7 **composition and the optical fitted kappa agree within uncertainties if we**
8 **assume the kappa from the organic portion of the aerosol is $k_{org} < 0.1$, which**
9 **is consistent with other work such as Good et al., Atmos. Chem. Phys., 10(7),**
10 **3189–3203, 2010.**

11
12 10. Page 3136, line 27-28: awkward phrasing “globally and over the SEUS” suggests that
13 the SEUS is not part of the globe. Suggest that this is re-phrased

14
15 **We have removed globally from the sentence it now reads: “Shallow cumulus**
16 **convection is common over the SEUS.”**

17
18 11. Page 3137, line 10-11: Does “mixed layer height” mean top of the mixed layer?
19 Please clarify.

20
21 **We have changed “mixed layer height” to “the top of the mixed layer” to**
22 **avoid any confusion.**

23
24 12. Figure 3 caption (and generally all Figures): please specify which variables are
25 measured and which are calculated.

26
27 **We have added more description to Figs. 3, 8, 9, and 10 so that it is clear to**
28 **the reader which quantifies are directly measured and which are calculated**
29 **from precursor measurements.**

30
31 13. Figure 4: It would be appropriate to use reduced major axis fitting here. Please
32 specify in the caption/text if this is the case or correct if otherwise.

33
34 **For this fit we have used orthogonal distance regression (ODR) and have**
35 **added this detail to the text. Using the ODR fit method is appropriate**
36 **because both independent and dependent variable are expected to have**
37 **similar uncertainty and the purpose of the fitting is to determine the**
38 **relationship between extinction aloft and on the surface.**

39
40 14. Page 3139, lines 21-22: ion charges missing on nitrate (NO₃⁻), ammonium (NH₄⁺),
41 and sulfate (SO₄²⁻)

42
43 **In the literature, we have found examples of AMS data presented with and**
44 **without the ion charges. We normally don't use the charges when referring**
45 **to AMS data, since those signals can originate from organic species in**
46 **addition to inorganic salts. For an example of AMS data presented without**

1 ion charges see Ng, et al., *Aerosol Science and Technology* 45(7), 770-784,
2 Figs. 7 and 9. Below is a passage from the text illustrating this point. We
3 have added the sentence in italics to inform the reader of the notation.

4 “The aerosol mass is the total of all ions measured by the AMS, and these
5 ions are typically classified as SO₄, NH₄, NO₃, and OA. The inorganic ions
6 are typically formed by ionization of simple salts such as ammonium sulfate
7 and ammonium nitrate or may be formed from more complex compounds (i.
8 e. organosulfates, organonitrates, and amines) that produce inorganic and
9 organic ions when ionized. *To indicate this complexity, we have omitted ionic*
10 *charges from the notation (i. e. SO₄, NH₄, NO₃).*”

11
12 15. Page 3141, line 14: “virtual potential temperature was constant”. With what
13 tolerance?

14
15 **We have added the tolerance to the text. The relevant sentence is copied**
16 **below.**

17
18 “For individual profiles, the mixed layer height was defined by inspection of
19 each profile as the highest altitude at which the virtual potential temperature
20 (Θ_v) was constant (typical variation in the mixed layer was less than 0.5 K)
21 and there was a reduction in the isoprene concentration.”

22
23 16. Section 4.1: Please comment on the impact of neglecting horizontal advection.

24
25 **We have added the following sentences to the Section 2.5 motivating the**
26 **aggregation of individual profiles.**

27
28 “Individual profiles are affected by horizontal advection which couples
29 spatially inhomogeneous emissions to the vertical profiles. Because of
30 vertical wind shear and spatial variability during slant profiles, the vertical
31 layers in an individual profile are not always directly comparable. The
32 aggregation the individual profiles is used to reduce the influence of this
33 variability and resolve the typical vertical structure and mixing over the
34 SEUS.”

35
36 17. Section 4.1: Could you comment on how/whether this analysis of the fraction of air is
37 affected by the lifetime of the assumed compound (i.e. CO) relative to the applied species
38 (i.e. aerosols)?

39
40 **For this analysis, the important time scale is that of atmospheric mixing. In**
41 **the mixed layer this time scale is approximately one half hour. In the**
42 **transition layer, the typical lifetime of a cumulus cloud is ~ 1 hour, so the**
43 **timescale for mixing in transition layer might be a few hours. Regional**
44 **subsidence (typical velocity = 500 meters /day) mixes air from the free**
45 **troposphere into the transition layer and mixed layer below. The lifetime of**
46 **both aerosol and CO are much longer than all of these lower troposphere**

1 **mixing processes. We could use other long lived species (CH₄, CO₂, non-**
2 **precipitating H₂O) to determine the fraction of air from the mixed layer,**
3 **$f_m(h)$, and Fig. 8 shows that the vertical profile of all of these long live species**
4 **behave in a similar manner.**

5
6 18. Page 3145, lines 23-24: How does the vertical profile of aerosol mass/extinction
7 differ when including biomass burning?
8

9 **During the SENEX study, the plumes from several small agricultural fires**
10 **were transected over the SEUS. These transects intentionally targeted these**
11 **plumes, and the plumes were transected during level flight legs. During**
12 **SEAC⁴RS, several large western wildfire plumes were sampled over the**
13 **western US (in research flights that were not used here) and several small**
14 **agricultural fires plumes were similarly sampled over the SEUS again largely**
15 **during level flight legs. Because the analysis presented here only considered**
16 **the ascending and descending portions of the flights, these biomass burning**
17 **plumes were *implicitly* not included in this analysis. Hence *explicitly***
18 **including/excluding these plumes has no effect on the analysis presented**
19 **here.**

20
21 **In the course of our analysis, we first explicitly excluded the biomass burning**
22 **transects from the data from each flight and then extracted the profiles.**
23 **However we subsequently realized that the biomass burning didn't occur**
24 **during the profiles. We have modified (copied below) the description of the**
25 **data filtering in Section 2.5 to indicate this point.**

26
27 **“Transects of biomass burning plumes were identified using tracers such as**
28 **the acetonitrile mixing ratio, were typically during level flight legs, and were**
29 **not found in any of the profiles used in this analysis.”**
30

31 19. Page 3147, line 15: typo: eq (5)

32
33 **We have corrected the equation referenced in this sentence to Eq. 5.**
34

35 20. Page 3147, line19-20: The authors might want to note that this approach is supported
36 by their own analysis in Figure 4.
37

38 **We have added a note that the assumption is supported by the correlation in**
39 **Fig. 4.**
40

41 **“Because extinction at the surface and aloft in the mixed layer are well**
42 **correlated as shown in Fig. 4, the dry extinction is extrapolated as a constant**
43 **to the surface based on the mean extinction measured in the lowest 200 m of**
44 **each profile.”**
45

46 21. Figure 11: caption missing (caption is for Figure 12).

1
2 **We have corrected this error. The caption for Fig. 11 follows below:**

3
4 **“Figure 11: Histograms of the transition layer enhancement ($E(h)$ – see Eq.**
5 **4) for several trace gases and aerosol properties. The first column shows**
6 **conserved species and black carbon: (A) CH₄, (B) CO₂, (C) H₂O, and (D)**
7 **black carbon mass. The second column shows the aerosol extensive**
8 **properties: (E) aerosol mass, (F) dry extinction, and (G) aerosol volume. The**
9 **third column shows the aerosol composition: (H) OA, (I) SO₄, (J) NH₄, and**
10 **(K) NO₃. The Student’s T-test and resulting p-value (noted in each**
11 **histogram) were used to test if the mean of each distribution was statistically**
12 **different from zero.”**

13
14 22. Figure 12: typo “total sulfur (tS).”

15
16 **We have corrected the labels on Fig. 12.**

17
18 Anonymous Referee #2 Received and published: 7 April 2015

19
20 This manuscript uses aircraft in-situ data from two different campaigns (SEAC4RS and
21 SENEX) during the summer and early fall of 2013. The aircraft platform has advantages
22 to other platforms (space and ground) in that vertical layers can be probed directly. The
23 analyses presented though representative of a small time period, are methodical and
24 logical. However, these results seem to be disconnected to other research in this area.
25 This reviewer kept waiting to read about how these results tie in (or do not tie in) with
26 other contextual works. The conclusion could potentially be quite insightful, if given the
27 proper context in which to state it. Overall, the work is sound and could be improved by
28 minor changes.

29
30 **We have made a few changes to the manuscript to provide the reader with**
31 **more context. First, we have added a figure which compares the AOD of**
32 **aircraft profiles to the AOD measured by sun photometer at two sites in the**
33 **SEUS. Second, we have added a brief discussion of two recent articles**
34 **relevant to the hypothesis of the layer aloft. The following sentences were**
35 **added to the conclusion.**

36
37 **“The hypothesis is partially supported by the spatial similarity of**
38 **summertime biogenic emission and summertime AOD over the SEUS.**
39 **Although, Alston et al. [2012] found that the spatial similarity depended on**
40 **the spatial resolution AOD of the data used in the analysis, and their analysis**
41 **of AOD and surface aerosol mass over Georgia did not fully support the**
42 **hypothesis. Kim et al. [2015] found that the increase of the planetary**
43 **boundary layer height during the summer could bring the seasonality of the**
44 **AOD and surface aerosol mass into agreement without the need for an**
45 **aerosol layer aloft. “**

1 Specific points:

2 1 - Section 3.1: Were there any other measurements that could be related to groundbased
3 measurements similar to Fig. 4 in Section 3.1. This could open up an avenue of
4 comparison with older field intensive studies in the same region, e.g., Atlanta Supersite
5 Experiment in 1999.

6
7 **Although detailed comparison of aircraft and surface measurements and**
8 **historical measurements are scientifically interesting and there is potentially**
9 **a lot that can be learn from them, aside from surface measurements**
10 **presented in section 3.1 (included to support assumptions used to calculate**
11 **AOD) they are beyond the scope of this analysis.**

12
13 2 - Typo: Line 9 3143 change expecting to expected

14
15 **We have corrected this typo.**

16
17 3 - Section 4.3: It would have been more conceptually thorough if the authors had
18 brought in some satellite (CALIPSO for vertical profile comparison, OMI as another
19 indicator of the lack of biomass burning aerosols) observation comparisons in Section
20 4.3. Even if that work is being done by another author, a reference to those results would
21 have been helpful to understand what dynamics the entire region was undergoing at the
22 time of these flights. Or the authors could have compared their results with time averaged
23 satellite information, which could open up the avenue for discussing how similar or
24 dissimilar summer 2013 was from other summers.

25
26 **We have added an additional figure and references to some complementary**
27 **work (see the response to the overview comments of the first and second**
28 **reviewers).**

29
30 4 - Section 4.3: There did not appear to be much summarization at the end of each
31 respective section. Is that on purpose? The only section that does an adequate job in
32 relating that section's work to the field at large is Section 4.3.

33
34 **This comment makes largely the same point as comment 5 and is addressed**
35 **in the response to that comment.**

36
37 5 - Conclusions: Most of this section speaks to the hypothesis of an elevated layer of
38 aerosols which account for changes in AOD and the author's perspective on that. What
39 about the other results? How do these other results shown in Figs 1-12 support the
40 author's thesis statement? There was a lot of work done to create these different analyses,
41 yet at the end there's scant mention of them.

42
43 **Many of the other results are included to support the conclusion of a modest**
44 **enhancement in the transition layer. For example Fig. 4, demonstrates that**
45 **aerosol is well mixed down to the surface below the minimum altitude of the**
46 **aircraft and that extinction can be extrapolated to the surface in the AOD**

1 calculation. Fig. 11 shows the statistical significance of the observed
2 enhancements. Figs. 8 and 12 are included to demonstrate that other long
3 lived species have a profile similar to CO. Fig. 12 also shows a reduction in
4 the precursor of particulate sulfate, SO₂, further supporting the observed
5 enhancement of particulate sulfate in the transition layer. In the conclusion,
6 rather than reiterating these supporting agreements we discuss the
7 disagreement between our observations and the hypothesized layer. To
8 explain how the absence of a large layer of enhanced aerosol in Fig. 3
9 motivated a more refined analysis, we have added a paragraph to the
10 conclusion to tie together the altitude-binned aggregate in Figs 3-5 with the
11 altitude-normalize aggregate presented in Figs. 7-10.

12
13 “Here, we have examined in situ vertical profiles of aerosol and found the
14 dry aerosol to be well mixed in the lowest layer. Above the lowest layer the
15 aerosol mass and extinction decreased with increasing altitude above that
16 layer (Figs. 3-5). The hygroscopic a growth of aerosol resulted in a layer of
17 enhanced extinction near the top of the mixed layer. The aerosol water
18 accounted for approximately a third of the AOD which would account for a
19 portion of the summertime AOD enhancement. The hypothesized, large
20 enhancement of secondary aerosol aloft was not apparent in these aggregate
21 profiles. However, after normalizing the altitude to the vertical structure
22 and using the CO concentration to quantify the vertical mixing during
23 shallow cumulus convection, we were able to resolve a modest enhancement
24 of aerosol in the transition layer.”

25
26 6 - Figures: Fig 13 is somewhat confusing. What does the blue portion of the figure
27 represent? A couple of sentences added to the caption would help orient the reader.

28
29 We have added the following sentences to the caption for Fig. 13.

30 “The idealized blue profile of extinction at the center of the figure shows the
31 vertical location of each contribution to AOD. The light blue area represents
32 the extinction of dry aerosol, and the darker blue area shows the
33 enhancement to aerosol water.”

34
35 Additional changes:

- 36 1) We changes the notation of the hygroscopicity parameter from κ to
37 κ_{opt} to avoid confusion with hygroscopicity derived from more direct
38 measurements of the diameter growth factor i. e. HTDMA.
39
40 2) We have added some more background detail on biomass burning in
41 the SEUS to section 3.2 as suggest by B. Yokelson (through personal
42 communication).

43 “Biomass burning is common in the SEUS during the fall, winter, and
44 spring, but is less common during the summer. Zhang et al. [2010]

1
2
3
4

found that in the summer of 2007 biomass burning contributed between 2 and 10% to measurements of PM_{2.5}.”

1 **In situ vertical profiles of aerosol extinction, mass, and**
2 **composition over the southeast United States during SENEX**
3 **and SEAC⁴RS: Observations of a modest aerosol enhancement**
4 **aloft**

5
6 N. L. Wagner^{1,2}, C. A. Brock¹, W. M. Angevine^{1,2}, A. Beyersdorf³, P. Campuzano-
7 Jost^{2,4}, D. Day^{2,4}, J. A. de Gouw^{1,2}, G. S. Diskin³, T. D. Gordon^{1,2}, M. G. Graus^{1,2*}, J. S.
8 Holloway^{1,2}, G. Huey⁵, J. L. Jimenez^{2,4}, D. A. Lack^{1,2}, J. Liao^{1,2}, X. Liu⁵, M. Z.
9 Markovic^{1,2**}, A. M. Middlebrook¹, T. Mikoviny⁶, J. Peischl^{1,2}, A. E. Perring^{1,2}, M. S.
10 Richardson^{1,2}, T. B. Ryerson¹, J. P. Schwarz^{1,2}, C. Warneke^{1,2}, A. Welti^{1,2,7}, A.
11 Wisthaler⁸, L. D. Ziemba³, D. M. Murphy¹

12
13 [1] NOAA Earth System Research Laboratory, 325 Broadway, Boulder, CO 80305, USA

14 [2] Cooperative Institute for Research in Environmental Sciences, University of
15 Colorado, Boulder, CO 80309, USA

16 [3] NASA Langley Research Center, MS 483, Hampton, VA 23681, USA

17 [4] Department of Chemistry and Biochemistry, University of Colorado, Boulder, CO
18 80309, USA

19 [5] School of Earth & Atmospheric Sciences, Georgia Institute of Technology, Atlanta,
20 GA 30332, USA

21 [6] Oak Ridge Associated Universities (ORAU), Oak Ridge, Tennessee, USA

22 [7] Institute for Atmospheric & Climate Science, Swiss Federal Institute of Technology,
23 Zürich, Switzerland

24 [8] Institute for Ion Physics and Applied Physics, University of Innsbruck,
25 Technikerstrasse 25, 6020 Innsbruck, Austria

26 [*] Now at Institute of Meteorology and Geophysics, University of Innsbruck, Austria

27 [**] Now at Air Quality Research Division, Environment Canada, Toronto, ON, Canada

28
29 Correspondence to: N. L. Wagner (nick.wagner@noaa.gov)

30
31 **Abstract:**

1 Vertical profiles of submicron aerosol ~~over the southeastern United States (SEUS)~~
2 ~~during the summertime~~ from in situ aircraft-based measurements were used to construct
3 aggregate profiles of chemical, microphysical, and optical properties. These vertical
4 profiles were collected over the southeastern United States (SEUS) during the summer of
5 2013 as part of two separate field studies: the Southeast Nexus (SENEX) study and the
6 Study of Emissions and Atmospheric Composition, Clouds, and Climate Coupling by
7 Regional Surveys (SEAC⁴RS). Shallow cumulus convection was observed during many
8 profiles. These conditions enhance vertical transport of trace gases and aerosol and
9 create a cloudy transition layer on top of the sub-cloud mixed layer. The trace gas and
10 aerosol concentrations in the transition layer were modeled as a mixture with
11 contributions from the mixed layer below and the free troposphere above. The amount of
12 vertical mixing, or entrainment of air from the free troposphere, was quantified using the
13 observed mixing ratio of carbon monoxide (CO). Although the median aerosol mass,
14 extinction, and volume decreased with altitude in the transition layer, they were ~10%
15 larger than expected from vertical mixing alone. This enhancement was likely due to
16 secondary aerosol formation in the transition layer. Although the transition layer
17 enhancements of the particulate sulfate and organic aerosol (OA) were both similar in
18 magnitude, only the enhancement of sulfate was statistically significant. The column
19 integrated extinction, or aerosol optical depth (AOD), was calculated for each individual
20 profile, and the transition layer enhancement of extinction typically contributed less than
21 10% to the total AOD. Our measurements and analysis were motivated by two recent
22 studies that have hypothesized an enhanced layer of secondary ~~organic aerosol (SOA)~~
23 aloft to explain the summertime enhancement of AOD (2-3 times greater than winter)
24 over the southeastern United States. The first study attributes the layer loft to secondary
25 organic aerosol (SOA) while the second study speculates that the layer aloft could be
26 SOA or secondary particulate sulfate. In contrast to ~~this~~ ~~these hypotheses~~ ~~hypothesis~~, the
27 modest enhancement we observed in the transition layer was not dominated by OA and
28 was not a large fraction of the summertime AOD.

30 1. Introduction

1 Shallow cumulus convection is common over the southeastern United States
2 (SEUS) during the summer. It enhances the vertical transport of trace gases and aerosol,
3 and creates a transition layer between the mixed layer and free troposphere [Siebesma,
4 1998]. Due to the presence of clouds and entrainment in the transition layer, it has also
5 been referred to as the cloud layer and the entrainment zone. The transition layer is
6 intermittently mixed by thermal plumes that originate in the mixed layer and form
7 cumulus clouds that release latent heat within the layer. There have been several
8 observations of vertical transport and redistribution of trace gases by shallow cumulus
9 convection [Angevine, 2005; Ching and Alkezweeny, 1986; Ching et al., 1988; Greenhut,
10 1986], and a few studies have investigated the vertical transport and aerosol formation
11 during cumulus convection [Ching et al., 1988; Sorooshian et al., 2007; Sorooshian et
12 al., 2006; Wonaschuetz et al., 2012].

13 Based on the seasonality of the surface aerosol-AOD relationship in the SEUS
14 and the spatial similarity of biogenic emissions and enhanced AOD, Goldstein et al.
15 [2009] and Ford and Heald [2013] have hypothesized the existence of a layer of enhanced
16 SOA secondary aerosol aloft in the summer which contributes to AOD but not to surface
17 measurements of aerosol mass. Goldstein et al. hypothesize that the aerosol layer is
18 primarily SOA, while Ford and Heald speculate that the layer aloft could be either SOA
19 or particulate sulfate. Although, neither study speculates about meteorological ~~and~~
20 ~~chemical~~ mechanisms that would lead to ~~its~~ the formation of this layer, aerosol
21 production in the transition layer of shallow cumulus convection is a plausible
22 mechanism that could produce the hypothesized layer. More generally, the vertical
23 distribution of aerosol and aerosol formation are integral to understand the relationship
24 between aerosol mass (PM_{2.5}) at the surface and AOD [Hoff and Christopher, 2009].

25 Submicrometer aerosol particles, which dominate aerosol mass, are largely
26 secondary and composed of OA and sulfates during the summer in the SEUS [Edgerton
27 et al., 2005; Weber et al., 2007]. While the formation mechanisms of secondary
28 particulate sulfate are well understood (e. g. Seinfeld and Pandis [1998]), the formation
29 of SOA is more complex and uncertain. Both biogenic and anthropogenic precursor
30 emissions are thought to be important [de Gouw and Jimenez, 2009]. The relative
31 importance of the homogenous and aqueous oxidation pathways for both sulfate and OA

1 is also uncertain [Carlton and Turpin, 2013; Carlton et al., 2008; Eatough et al., 1994;
2 Ervens et al., 2011; Luria and Sievering, 1991; McKeen et al., 2007]. Based on the
3 abundance of aerosol water and cumulus convection, aqueous processing is expected to
4 be an important aerosol formation pathway in the SEUS [He et al., 2013], and processing
5 in cloud droplets would occur primarily in the transition layer.

6 In this analysis, aircraft-based in situ measurements of aerosol chemical, physical,
7 and optical properties are used to examine the vertical structure of aerosol in the SEUS
8 during shallow cumulus convection and to quantify aerosol enhancements in the
9 transition layer and its contribution to summertime AOD. We use measurements made
10 aboard the National Oceanic and Atmospheric Administration (NOAA) WP-3D aircraft
11 during the ~~NOAA Southeast Nexus (SENEX)~~ study in June and July of 2013 and the
12 National Aeronautic and Space Administration (NASA) DC-8 aircraft during ~~the Study~~
13 ~~of Emissions and Atmospheric Composition, Clouds, and Climate Coupling by Regional~~
14 ~~Surveys (SEAC⁴RS)~~ in August and September of 2013 to construct aggregate vertical
15 profiles of aerosol extinction, mass, and composition as a function of altitude over the
16 SEUS. The transition layer aerosol and trace gas concentrations are modeled as a
17 mixture with contributions from the free troposphere and mixed layer. The in situ
18 measurements of the extinction coefficient are used to calculate the AOD and
19 contributions to the AOD from aerosol water, from the mixed layer, and from the
20 transition layer.

21

22 **2. Methods and Measurements**

23 In this analysis we combine data collected during two aircraft field studies that were
24 partially conducted over the SEUS in the spring and summer of 2013. Although the
25 SENEX study collected measurements in late spring and early summer while SEAC⁴RS
26 collected measurements in the late summer, both studies encountered shallow cumulus
27 convection. Additionally, both aircraft hosted a similar set of in situ instruments which
28 was conducive to a combined analysis.

29

30 **2.1 SENEX**

1 The SENEX study was part of the larger Southeast Atmosphere Study (SAS) in the
 2 SEUS during the June and July of 2013. The NOAA WP-3D aircraft flew 18 research
 3 flights based out of Smyrna, Tennessee during June and July 2013 for SENEX with a
 4 payload of instruments measuring atmospheric trace gases, aerosol properties, and
 5 meteorological parameters. This analysis uses measurements of carbon monoxide (CO),
 6 carbon dioxide (CO₂), methane (CH₄), sulfur dioxide (SO₂), isoprene, aerosol
 7 composition, and aerosol optical properties (Table 1). The aerosol was sampled
 8 downstream of a low turbulence inlet [Wilson *et al.*, 2004] and an impactor with a 1 μm
 9 aerodynamic diameter size cut. Before impactation, the sampled aerosol was initially dried
 10 by ram heating when sampling into the aircraft. The sampled aerosol was then dried
 11 further in each instrument.

12 The non-refractory aerosol composition was measured by a compact time-of-flight
 13 aerosol mass spectrometer (AMS) downstream of a pressure controlled inlet [Bahreini *et*
 14 *al.*, 2008] and most (97%) of the submicron volume measured by the aerosol sizing
 15 instruments was transmitted into the AMS during SENEX. The collection efficiency for
 16 the AMS was determined by the composition for each data point using the algorithm
 17 described by Middlebrook *et al.* [2012]. When comparing the volume derived from
 18 composition (AMS plus black carbon mass) to the volume measured by the aerosol sizing
 19 instruments in the manner outlined by Bahreini *et al.* [2009], 87% of the aerosol
 20 composition and sizing data from the entire SENEX study are within the combined
 21 uncertainties.

22
 23 **Table 1:** Measurements aboard the NOAA WP-3D used in this analysis. The sample
 24 interval corresponds to the rate at which data is reported and is the integration time for
 25 the lower limit of detection.

Measurement	Technique	Sample Interval	Lower Limit of Detection	Accuracy	Reference
<u>Dry Sub-micrometer Aerosol Extinction (532 nm)</u>	Cavity Ringdown Spectrometer	1 s	0.1 Mm ⁻¹	5% (RH < 30%)	[Langridge <i>et al.</i> , 2011]
<u>Humidified Sub-micrometer Aerosol Extinction (532 nm)</u>	Cavity Ringdown Spectrometer	1 s	0.1 Mm ⁻¹	11% (RH = 90%)	[Langridge <i>et al.</i> , 2011]
Sub-micrometer Aerosol Composition	Compact – Time of Flight – Aerosol Mass Spectrometer	10 s	OA < 0.8-4 μg m ⁻³ SO ₄ < 0.4-0.5 μg m ⁻³	38% OA 34% Inorg 35%	[Drewnick <i>et al.</i> , 2005], [Canagaratna <i>et al.</i> , 2007]

Sub-micrometer Aerosol Volume	Optical particle counter	1 s	0.03 $\mu\text{m}^3 \text{cm}^{-3}$	+26%, -12 %	[Cai <i>et al.</i> , 2008]
CO	Vacuum UV -Ultraviolet fluorescence	1 s	0.5 ppbv	5%	[Holloway <i>et al.</i> , 2000]
Isoprene	PTR-MS Proton Transfer Reaction Mass Spectrometer	14 s	< 32 pptv	20%	[de Gouw and Warneke, 2007]
RH (Dew Point (RH))	Chilled Mirror Hygrometer	1 s	-	0.2°C	-
Black Carbon Mass	SP2 Single Particle Soot Photometer	1 s	12 ng m^{-3}	30%	[Schwarz <i>et al.</i> , 2008]
SO ₂	Pulsed UV -Ultraviolet Fluorescence	1 s	250 pptv	20%	[Ryerson <i>et al.</i> , 1998]
CH ₄	Cavity Ringdown Spectrometer	1 s	-	1.2 ppbv	[Peischl <i>et al.</i> , 2012]
CO ₂	Cavity Ringdown Spectrometer	1 s	-	0.15 ppmv	[Peischl <i>et al.</i> , 2012]

1

2 2.2 SEAC⁴RS

3 SEAC⁴RS consisted of measurements aboard three aircraft based in Houston,
 4 Texas during August and September of 2013. In this analysis, we focus on in situ
 5 measurements from the NASA DC-8 aircraft, which conducted 19 research flights. The
 6 measurements that were collected onboard the DC-8 and used in this analysis are
 7 summarized in Table 2. Unlike the SENEX study, there was no continuous measurement
 8 of methane during SEAC⁴RS. The aerosol extinction and black carbon instruments
 9 flown on the DC-8 during SEAC⁴RS were the same instruments used onboard the NOAA
 10 WP-3D aircraft during SENEX. Measurements of aerosol extinction, volume, black
 11 carbon mass sampled aerosol through a shrouded diffuser inlet described by McNaughton
 12 et al. [2007]. The aerosol extinction was measured downstream of 1 μm impactor.

13 The non-refractory aerosol composition was measured by a high resolution time-
 14 of-flight~~The aerosol mass spectrometer (AMS)~~ similar to the compact time-of-flight
 15 AMS used during the SENEX study. The two instrument differed in the resolution of the
 16 mass spectrometer. The higher resolution AMS used during SEAC⁴RS was operated
 17 with a 1 s sample interval. This AMS was operated similar to Dunlea et al. [2009] and
 18 also used a pressure-controlled inlet [Bahreini et al., 2008]. The composition-dependent
 19 formulation of Middlebrook et al. [2012] was used to estimate the collection efficiency.
 20 The AMS sampled aerosol downstream of ~~sampled aerosol through a~~ HIMIL inlet.
 21 ~~inlet~~ (<http://www.eol.ucar.edu/homes/dcrogers/Instruments/Inlets/>). In both ~~inlets~~ the

Formatted: Superscript

1 [HIMIL inlet and the shrouded diffuser inlet](#), the sampled aerosol was initially dried by
 2 ram heating and then further dried in each instrument.

3
 4 **Table 2:** Measurements aboard the NASA DC-8 used in this analysis. [The sample](#)
 5 [interval corresponds to the rate at which data is reported and is the integration time for](#)
 6 [the lower limit of detection.](#)

Measurement	Technique	Sample Interval	Lower Limit of Detection	Accuracy	Reference
Dry Sub-micrometer Aerosol Extinction (532 nm) (dry)	Cavity Ringdown Spectrometer	1 s	0.1 Mm ⁻¹	5% (RH < 30%)	[Langridge et al., 2011]
Humidified Sub-micrometer Aerosol Extinction (532 nm)	Cavity Ringdown Spectrometer	1 s	0.1 Mm ⁻¹	11% (RH = 90%)	[Langridge et al., 2011]
Sub-micrometer Aerosol Composition	High Resolution - Time of Flight – Aerosol Mass Spectrometer	1 s	OA-0.6 µg m ⁻³ OA SO ₂ -0.06 µg m ⁻³ SO ₄ NO ₂ -0.06 µg m ⁻³ NO ₂ NH ₄ -0.01 µg m ⁻³ NH ₄	35% 38% OA 34% Inorg.	[Canagaratna et al., 2007]
Sub-micrometer Aerosol Volume	Optical particle counter	1 s	0.03 um ³ cm ⁻³	+26%, -12 %	[Cai et al., 2008]
CO	Infrared Absorption	1 s	0.5 ppbv	5%	[Sachse et al., 1987]
Isoprene	Proton Transfer Reaction Mass Spectrometer PTR-MS	14 s	25 pptv	10%	[de Gouw and Warneke, 2007]
RH (dew point) Dew Point (RH)	Chilled Mirror Hygrometer	1 s	-	0.2°C	-
Black Carbon Mass	SP2 Single Particle Soot Photometer	1 s	12 ng m ⁻³	30%	[Schwarz et al., 2008]
SO ₂	CIMS Chemical Ionization Mass Spectrometer	1 s	9 pptv	15%	[S Kim et al., 2007]
CO ₂	Infrared Absorption	1 s	-	0.2 ppm	[Vay et al., 2011]

7 8 2.3 Surface Measurements

9 The Southeastern Aerosol Research and Characterization (SEARCH) Network
 10 consists of 8 continuous monitoring ground sites in Georgia and Alabama hosting several
 11 gas-phase and aerosol measurements [Edgerton et al., 2005; 2006; Hansen et al., 2003].
 12 During SENEX the NOAA WP-3D flew over four of these sites a total of 15 times, and
 13 extinction near the surface is calculated using measurements of aerosol scattering
 14 (Radiance Research Model M903 nephelometer, Tempe, Arizona, USA) and absorption
 15 (Magee Scientific Model AE-16 Aethalometer, Berkeley, California, USA) at each SEARCH

1 site to compare with the extinction measured onboard the NOAA WP-3D aircraft in the
2 mixed layer.

3

4 **2.4 Aerosol Water**

5 The enhancement of extinction due to condensation of water onto the aerosol is
6 modeled using an empirical parameterization (shown in Eq. 1), hereafter referred to as
7 the kappa parameterization [Brock *et al.*, in preparation]. The hygroscopic growth of
8 particle diameter is described by kappa-Kohler theory [Petters and Kreidenweis, 2007].
9 A particle size distribution and a Mie scattering calculation would be necessary to
10 rigorously extend the kappa-Kohler theory to the hygroscopic enhancement of optical
11 properties. However, Brock *et al.* [in preparation] shows that if atmospheric
12 accumulation mode size distributions typical of the SEUS are used, the functional form of
13 kappa-Kohler theory can be applied directly to the optical extinction (Eq. 1).

14

$$15 \quad \sigma_{ext}(RH) = \sigma_{ext}(dry) \times \left(1 + \kappa_{opt} \times \left(\frac{RH}{100 - RH} \right) \right) \quad (1)$$

16

17 The humidified extinction coefficient $\sigma_{ext}(RH)$ is a function of the dry extinction $\sigma_{ext}(dry)$
18 and the hygroscopicity parameter κ_{opt} . We note that κ_{opt} is based on the measurement of
19 humidified extinction rather than the direct measurement of the diameter growth factor or
20 activation fraction, i. e. humidified tandem differential mobility analyzers (HTDMA) and
21 cloud condensation nuclei counters (CCNc). The aerosol extinction is measured in three
22 separate constant RH channels: in dry conditions (RH less than 30%), medium RH
23 typically 70%, and high RH greater than 80%. The hygroscopicity parameter (κ_{opt}) is
24 determined by fitting the three measurements of extinction to Eq. 1. The resulting
25 κ_{opt} and $\sigma_{ext}(dry)$ are then used to estimate the extinction at ambient RH. Lower values
26 of aerosol hygroscopicity generally correspond to mineral dust, aerosol with high soot
27 fraction, or primary OA such as fresh biomass burning emissions or automotive
28 emissions [Massoli *et al.*, 2009; Quinn *et al.*, 2005]. High hygroscopicity usually
29 corresponds to an oxidized, aged aerosol, large sulfate mass fractions and/or sea salt
30 aerosol.

1 The calculated ambient extinction ~~is a lower limit of~~ will differ from the actual
2 ambient extinction in three cases. First, if the hygroscopic growth exhibits hysteresis and
3 the ambient RH is below the deliquesce RH, ambient particles may be on the
4 deliquescing (lower) or efflorescing (upper) branch of the hysteresis curve [*Santarpia et*
5 *al.*, 2004]. Our extinction measurements ~~cannot~~ distinguish between these two states,
6 because ~~the sample aerosol is first dried, and then re-~~ Then the aerosol is humidified to
7 RH greater than 90% in a cooled Nafion humidifier. The temperature of the humidifier
8 (10-15 K below instrument temperature for 70% RH and 1-3 K below for 90% RH) is
9 varied to control amount of water vapor added to the sample and maintain a constant RH
10 in the sample cell. Finally the sample aerosol is reheated to the instrument temperature
11 and measured in the sample cell, in our instrument before measurement at high RH. (The
12 sample aerosol is exposed to elevated RH for a duration of 4 s before measurement.)

13 Hence, the measured extinction at high RH and the subsequently calculated
14 hygroscopicity parameter κ_{opt} represent the hygroscopic growth of an
15 ~~efflorescing/deliquescing~~ aerosol on the ~~lower~~ upper branch. If the aerosol undergoes
16 hysteresis, we expected most aerosol in the summertime SEUS to be on the upper branch
17 because the aerosol regularly pass through clouds and are exposed to high RH conditions.
18 The aerosol also rarely experience dry conditions (RH less than 30%). Second, because
19 the kappa parameterization produces an ambient extinction that asymptotically
20 approaches infinity as RH approaches 100%, we used ambient RH to calculate the
21 ambient extinction only when RH was less than 95%, and assumed a constant RH of 95%
22 when ambient RH was greater than or equal to 95%. Therefore, the calculated ambient
23 extinction is a lower limit of the ambient extinction when RH was greater than 95%.
24 Third, in the case that super-micrometer particles (which are not sampled by instruments
25 used in this analysis) make a significant contribution, the ambient extinction is
26 underestimated. This is typically the case during dust events and during in-cloud
27 sampling which were either not observed or excluded from this analysis, respectively.
28

29 2.5 Aggregation of Vertical Profiles

30 Individual profiles are affected by horizontal advection which couples spatially
31 inhomogeneous emissions to the vertical profiles. Because of vertical wind shear and

Formatted: Subscript

1 spatial variability during slant profiles, the vertical layers in an individual profile are not
2 always directly comparable. The aggregation the individual profiles is used to reduce the
3 influence of this variability and resolve the typical vertical structure and mixing over the
4 SEUS. For this analysis, individual-Individual vertical profiles were selected from the
5 research flights by inspection of the altitude time series and are generally included for all
6 ascents and descents with an altitude difference greater than 1 km. Measurements during
7 level flight legs were not used in this analysis. Although cloud penetration was mostly
8 avoided, aerosol data sampled during cloud penetration events were excluded due to the
9 effects of particle shattering in the inlets. Cloud penetration events were identified using
10 the video from the nose of the aircraft and cloud particle imaging probes mounted near
11 the wingtips. Transects of biomass burning plumes were identified using tracers such as
12 the acetonitrile mixing ratio ~~and, were typically during level flight legs, and were not~~
13 ~~found during any of the profiles used in this analysis-were excluded from the analysis.~~
14 Extensive aerosol parameters (mass, extinction, volume) have been corrected to standard
15 temperature (0 °C) and pressure (1 atmosphere). All calculated quantities such as
16 ambient extinction and transition layer enhancements were determined before
17 aggregation and then were aggregated in the same manner as the observations.

18 For the SENEX campaign, the vertical profiles (which were located primarily over
19 northern Georgia and Alabama) were generally included in the flight plans for three
20 purposes: to characterize the background boundary layer structure before and after urban
21 and power plant plume intercepts, to characterize the vertical structure over surface
22 measurement sites, and as enroute ascents and descents into and out of the region of
23 interest. The SEAC⁴RS profiles that we use were distributed through Mississippi and
24 Alabama and were conducted to characterize inflow and outflow near convective
25 systems, to examine boundary layer chemistry over the SEUS, and as enroute ascents and
26 descents. The individual vertical profiles used here include both spiral and slant ascents
27 and descents and were typically between 5 and 15 min. in duration.

28 In this analysis we construct two types of aggregate profiles, the first of which
29 includes all of the afternoon vertical profiles over the SEUS and is binned according to
30 altitude above ground level ("altitude-binned" aggregate profiles). The second type of
31 aggregate includes only the subset of profiles during which shallow cumulus convection

1 was present and is binned according to a normalized altitude described in Sec. 3.2
2 ("normalized" aggregate profiles). The profiles not included in the normalized
3 aggregates were either collected during deeper convection and/or had a more complicated
4 structure.

5 For the altitude-binned profiles, we have chosen all of the available vertical
6 profiles from both SENEX and SEAC⁴RS over Mississippi, Alabama, and Georgia in the
7 afternoon between 12:00 pm and 6:30 pm Central Daylight Time (CDT) when we expect
8 the boundary layer structure to be well developed and no residual layers left over from
9 the previous day. The aggregate includes 74 profiles of which 41 profiles are from 6
10 research flights during SENEX and 33 profiles from 6 research flights during SEAC⁴RS.
11 The locations of the profiles used in the altitude-binned aggregate are shown in Fig. 1.
12 The data from individual vertical profiles were aggregated into 150 m vertical bins from
13 the surface to 4.5 km based on the altitude above ground level. The vertical bin height of
14 150 m was chosen such that the slower measurements (aerosol mass and isoprene)
15 typically contributed at least one datum to each bin for each individual profile. In each
16 bin with data from 5 or more individual profiles, the median, interquartile range, and
17 interdecile range were calculated. The median and percentiles were used because these
18 statistics are more robust when outliers are present. The number of vertical profiles
19 which contribute to each aggregated altitude bin varies with altitude because of the
20 differences of the starting and ending altitudes of each individual profile (Fig. 2a).
21 During some profiles or some portions of a profile, individual measurements of trace
22 gases and aerosol properties did not report data (e. g. due to zeroing or calibrations).

23 The normalized aggregate profiles were calculated using only those individual
24 profiles obtained during shallow cumulus convection and were altitude-normalized as
25 described below. Shallow cumulus convection is common ~~globally and~~ over the SEUS.
26 Warren et al. [2007] have compiled a global cloud climatology based on surface
27 observations. According to their work, the mean frequency of daytime cumulus clouds is
28 49% over Alabama during June, July, and August, and the mean cloud coverage when
29 cumulus clouds are present is 35%. The presence of shallow cumulus convection during
30 individual profiles was determined by inspection of visible images from the GOES
31 satellite and the presence of a three layer structure (mixed layer, transition layer, and free

1 troposphere), which is expected during shallow cumulus convection. The second
2 aggregate includes 37 of the 74 SEUS profiles from the first aggregate. The locations of
3 profiles in the second aggregate are show in Fig. 1, and Fig. 2b shows the distributions of
4 the mixed layer and transition layer heights determined from individual profiles which
5 had medians of 1.2 km and 2.2 km respectively. For cumulus convection the height of
6 the planetary boundary layer is defined as the cloud base or the top of the mixed
7 layer~~mixed layer height~~; however, we find the term planetary boundary layer confusing
8 in the context of shallow cumulus convection and have avoided using it. Determination
9 of the mixed layer height and transition layer height is described in Sec. 3.2. For the
10 normalized aggregate profiles, there are 25 bins assigned to each layer. Figure 2c shows
11 the number of profiles that contribute to the second aggregate at each normalized altitude.
12 The number of profiles varies with normalized altitude due to variability in the starting
13 and ending altitudes of each profile and because the second aggregate is limited to
14 portions of the individual profiles when aerosol mass, extinction, volume and CO
15 measurements all report data. Limiting data as such facilitates quantitative comparison of
16 the aggregate profiles. In contrast the first aggregate is constructed using all available
17 data.

18

19 **3. Results**

20

21 **3.1 Altitude-Binned Aggregate Profile**

22 Altitude-binned aggregate profiles of dry and ambient aerosol extinction show
23 several characteristics of note (Fig. 3). The median 532 nm dry extinction coefficient
24 (Fig. 3a) is approximately independent of altitude below 1.5 km with median value of 50
25 Mm^{-1} , and the interquartile range is 27 Mm^{-1} to 73 Mm^{-1} . The interquartile (25th -75th
26 percentiles) and interdecile (10th – 90th percentiles) range are due largely to variation
27 between individual profiles rather intra-profile point-to-point variation. Above 1.5 km
28 the extinction coefficient decreases with altitude to a median value of 6 Mm^{-1} above 3.0
29 km. The gradual decrease in extinction with altitude from 1.2 to 2.5 km is due to the
30 variation of mixed layer and transition layer heights in the individual profiles. Figure 3b
31 shows the RH increasing with increasing altitude below 1.2 km. Above this level the RH

1 has a slight decreasing trend with altitude and a large interquartile range spanning 30-
2 70%. The relative humidity of the aggregate profile could be biased low, because during
3 SENEX the flight dates were chosen to avoid precipitation and cloud penetration was
4 mostly avoided during flights however this was not the case during SEAC⁴RS.

5 The median hygroscopicity parameter (κ , Fig. 3c) increases from 0.11 at the
6 bottom of the profile to 0.18 at 3 km and is more variable above 3 km. The hygroscopic
7 growth of the aerosol enhances the ambient extinction (Fig. 3d) throughout the profile
8 and significantly between 0.7 and 1.7 km. Below 1.2 km, the ambient extinction
9 coefficient increases with altitude due to increasing RH, and above 1.2 km decreases with
10 altitude due to a combination of decreasing RH and decreasing dry extinction. The
11 hygroscopic growth of aerosol and the subsequent enhancement of extinction aloft could
12 explain some of the enhancement of AOD noted by Goldstein et al. [2009] and Ford and
13 Heald [2013].

14 The minimum altitude of individual aircraft profiles ranged from 300 - 700 m
15 above the surface. We estimate the profile of dry extinction between the surface and the
16 minimum altitude of the profiles by combining aircraft measurements made in the mixed
17 layer in the vicinity of surface monitoring sites using ground data from those sites.
18 During the SENEX study, there were 15 overflights in the mixed layer within 10 km of
19 four SEARCH monitoring sites. The surface aerosol extinction at each SEARCH site
20 was calculated using the aerosol scattering coefficient measured by a nephelometer with a
21 center wavelength of 530 nm and the aerosol absorption coefficients measured by an
22 aethalometer at 880 nm. Because the optical absorption at this wavelength was likely due
23 to black carbon aerosol, we corrected the absorption coefficient to 530 nm using an
24 Ångstrom exponent of 1 which is conventionally used for black carbon [Bergstrom et al.,
25 2002; Lack and Langridge, 2013]. Absorption typically accounted for less than 5% of
26 the extinction. The calculated 530 nm surface extinction was not corrected to the 532 nm
27 aircraft extinction because the correction would be less than 1%. The surface and aircraft
28 extinction coefficients are correlated ($R^2 = 0.91$), and the slope of a ~~linear least~~
29 ~~squares~~ orthogonal distance regression (ODR) fit to the data indicates that the aircraft data
30 are ~6% lower than the surface measurements (Fig. 4), which is within the combined
31 uncertainty in the measurements. We conclude that the dry extinction is roughly

1 independent of altitude from the surface to the top of the well-mixed layer. Crumeyrolle
2 et al. [2014] found similar agreement between surface and aircraft-based boundary layer
3 measurements of ozone in the Baltimore-Washington metropolitan area.

4 The altitude-binned aggregate vertical profile of aerosol mass (Fig. 5a) is similar
5 in shape to the dry extinction profile. The median mass is $13.7 \mu\text{g m}^{-3}$ at the bottom of
6 the profile and decreases to $2.1 \mu\text{g m}^{-3}$ above 3 km. The aerosol mass is the total of all
7 ions measured by the AMS, and these ions are typically classified as SO_4 , NH_4 , NO_3 , and
8 OA. The inorganic ions may be typically represent-formed by ionization of simple
9 inorganic salts such as ammonium sulfate and ammonium nitrate in the aerosol or but may
10 be formed from more complex compounds with both an inorganic and organic character
11 (i. e. organosulfates, organonitrates, and amines) that produce both inorganic and organic
12 ions when ionized. To indicate this complexity, we have omitted ionic charges from the
13 notation (i. e. SO_4 , NH_4 , NO_3). In this classification scheme, the composition (Fig. 5b)
14 of the submicron aerosol is primarily OA, sulfate, and ammonium. The mass fraction of
15 the inorganic components (NO_3 , NH_4 , and SO_4) increase with altitude up to 3 km, while
16 the OA mass fraction decreases with altitude up to 3 km. Above 3 km, the OA fraction
17 increases; however, at this altitude the median aerosol mass is only $2 \mu\text{g m}^{-3}$. The
18 increase of aerosol hygroscopicity with altitude up to 3 km corresponds with the
19 increasing inorganic fraction of the aerosol. In particular, sulfate is typically more
20 hygroscopic than OA, is 20% of the aerosol mass at the bottom of the profile, and is 28%
21 of the aerosol mass at 3 km.

22 23 **3.2 Normalized Aggregate Profiles**

24 The heights of the mixed and transition layers varies among individual vertical
25 profiles and this variation obscures the transition layer in the altitude-binned aggregate
26 profile presented in Figs. 3 and 5. For example, the layer structure is clear in a semi-rural
27 profile measured in the vicinity of shallow cumulus convection over central Georgia on
28 the afternoon of 16 June (Fig. 6). The mixed layer is closest to the surface, a transition
29 layer is formed above the mixed layer, and the free troposphere is on top.

30 The layered structure is evident in both the physical parameters such virtual
31 potential temperature (θ_v) and ambient temperature as well as chemical mixing ratios

1 such as carbon monoxide (CO) and isoprene. In the mixed layer, adiabatically conserved
2 parameters such as virtual potential temperature (Fig. 6a) are independent of altitude.
3 However, in the transition the virtual potential temperature increases with altitude until
4 the top of the transition layer is reached where a capping temperature inversion is present.
5 In the mixed layer, the mixing ratio of water vapor is also independent of altitude;
6 however, RH increases with altitude as temperature decreases (Fig. 6b). Relative
7 humidity is high in the transition layer, and video from the nose of the aircraft confirms
8 the presence of clouds in this layer.

9 The transition layer is also evident in the comparison of long-lived trace gases
10 such as CO (Fig. 6c) with short lifetime trace gases such as isoprene (Fig. 6d). Carbon
11 monoxide is directly emitted during combustion, produced by oxidation of hydrocarbons,
12 lost to oxidation by OH, and typically has an atmospheric lifetime of 1 - 4 months which
13 varies seasonally and regionally [Seinfeld and Pandis, 1998]. In this profile, the CO
14 mixing ratio is greater than 110 ppbv in both the mixed and transition layers and
15 decreases to less than 100 ppbv in the free troposphere. In the mixed layer the CO
16 mixing ratio is independent of altitude and decreases modestly with altitude in the
17 transition layer. Isoprene is a short-lived trace gas that typically has an atmospheric
18 lifetime less than 2 hr. [Seinfeld and Pandis, 1998] and in the summertime is emitted by
19 vegetation common in the SEUS. In the mixed layer, the isoprene mixing ratio is greater
20 than 1 ppbv and variable due to heterogeneous surface emissions (Fig. 6d). The isoprene
21 mixing ratio in the transition layer is always less than 500 ppbv and typically ~10% of the
22 mixed layer value. In the free troposphere, the isoprene mixing ratio is below the
23 detection limit of the measurement.

24 To examine vertical structure in more detail, altitude-normalized aggregate
25 profiles were calculated. Altitude normalization is commonly done by dividing the
26 altitude by the height of the mixed layer. However, because of the more complex vertical
27 structure often encountered during shallow cumulus convection, we have defined a
28 normalized altitude, h_{norm} , for each profile such that the top of the mixed layer, h_{ML} , is
29 assigned a normalized altitude of 1, and the top of the transition layer, h_{TL} , is assigned a
30 normalized altitude of 2:

31

$$\begin{aligned}
1 \quad & 0 < h < h_{ML} & h_{norm} &= h / h_{ML} \\
2 \quad & h_{ML} < h < h_{TL} & h_{norm} &= 1 + (h - h_{ML}) / (h_{TL} - h_{ML}) \\
3 \quad & h > h_{TL} & h_{norm} &= 1 + h / h_{TL}
\end{aligned} \tag{2}$$

4

5 For individual profiles, the mixed layer height was ~~defined~~determined by inspection of
6 each profile as the highest altitude at which the virtual potential temperature (Θ_v) was
7 constant (typical variation in the mixed layer was less than 0.5 K) and there was a
8 reduction in the isoprene concentration. The top of the transition layer was defined by a
9 temperature inversion and a rapid decrease in the CO mixing ratio.

10 The altitude-normalized aggregate profiles of CO (Fig. 7a) and isoprene (Fig. 7b)
11 mixing ratios demonstrate the contrast between the mixed layer and transition layer.
12 During shallow cumulus convection, CO is transported out of the mixed layer into the
13 transition layer due to its longer lifetime relative to isoprene. The modest decrease of CO
14 with altitude in the mixed layer is likely due to the influence of near source emissions in
15 some profiles. In the mixed layer the isoprene profile is variable, and the median is only
16 modestly dependent on altitude with a median mixing ratio of 1 ppbv. However, the
17 median isoprene mixing ratio decreases to ~10% of this value in the transition layer. The
18 isoprene observed above the mixed layer is consistent with large eddy simulations
19 performed by Kim et al. [2012] who found that cumulus clouds can transport some
20 isoprene out of the mixed layer into the cloud layer.

21

22 **4. Analysis**

23

24 **4.1 Aerosol enhancements in the transition layer**

25 During shallow cumulus convection, the air in the transition layer is a mixture of
26 air from the mixed layer below and the free troposphere above. The concentrations of
27 trace gases and extensive aerosol parameters $C(h)$ in the transition layer are described in
28 this analysis by a vertical mixing model consisting of three terms (Eq. 3): a contribution
29 from the mixed layer, a contribution from the free troposphere, and any enhancement
30 $E(h)$ relative to concentration expected from the vertical mixing alone, as

1
2

$$C(h) = C_{ML}f_m(h) + C_{FT}(1 - f_m(h)) + E(h), \quad (3)$$

3

4 where $C(h)$ is the aerosol or trace gas concentration, C_{ML} and C_{FT} are the aerosol or trace
5 gas concentrations in the mixed layer and the free troposphere. Positive enhancements
6 could be due to local production, or direct emissions to the transition layer from buoyant
7 plumes, e. g. large biomass burning sources, and negative enhancements represent losses.
8 The fraction of air from the mixed layer (f_m) present in the transition layer is determined
9 by using the CO mixing ratio as

10

$$f_m(h) = \frac{CO(h) - CO_{FT}}{CO_{ML} - CO_{FT}}, \quad (4)$$

11

12
13 for which the enhancement $E(h)$ due to local production and losses is assumed to be
14 zero. For each profile, the mixing ratio of CO in the mixed layer CO_{ML} and the free
15 troposphere CO_{FT} were determined using the mean between normalized altitudes of 0.5
16 and 0.9 for the mixed layer and 2.0 and 2.5 for the free troposphere. To investigate
17 transition layer enhancements of chemical concentrations and aerosol extensive
18 properties, we calculate a concentration expected from vertical mixing alone using Eq. 3
19 and setting $E(h)$ to zero. The concentration expected from vertical mixing alone is
20 calculated for each profile and aggregated in the same manner as the observations. In the
21 Figs. 8-10, the median concentration expected from vertical mixing alone is shown as a
22 dashed line on top of the observed concentrations. The interquartile and interdecile
23 ranges of the value ~~expecting-expected~~ from mixing are not shown.

24 CO is produced through the oxidation of VOCs, and this CO production likely
25 accounts for a significant fraction of the CO budget during the summer in the SEUS
26 [Hudman *et al.*, 2008]. If CO production in the transition layer is significant, the fraction
27 of air from the mixed layer (f_m , determined using CO) would be biased high and any
28 transition layer enhancements of other species ($E(h)$, determined using the CO
29 concentration and Eqs. 3 and 4) would be biased low. By comparing the observed

1 concentration and the concentration expected from vertical mixing alone of several long
2 lifetime species, the importance of CO production in the transition layer can be assessed.

3 Fig. 8a shows the altitude normalized profile of the fraction of air from the mixed
4 layer (f_m , calculated using Eq. 4). The median is 1 in the mixed layer, 0 in the free
5 troposphere, and decreases from 1 to 0.6 in the transition layer due to entrainment of air
6 from the free troposphere. Figs. 8b-e show the altitude-normalized aggregate profiles
7 and the median concentration expected from vertical mixing alone (dashed line) of
8 methane (CH₄), carbon dioxide (CO₂), water vapor (H₂O), and black carbon aerosol
9 mass, respectively. Both CH₄ and CO₂ have atmospheric lifetimes greater than a year
10 and no significant production or losses in the transition layer on the time scale of
11 atmospheric mixing. (The aggregate profile in Fig. 8b only includes data from the
12 SENEX study because CH₄ was not measured during SEAC⁴RS.) H₂O and black carbon
13 aerosol are also not produced in the transition layer and are not lost except in the presence
14 of precipitating clouds. Profiles in precipitating clouds are mostly excluded from the
15 aggregate. Based on the agreement between the observed vertical profiles of CH₄, CO₂,
16 H₂O, and black carbon mass (Fig. 8) and their expected concentration from vertical
17 mixing alone, we conclude the CO production in the transition layer is not significant.

18 In contrast, the altitude-normalized profiles of submicrometer aerosol mass (Fig.
19 9a), extinction (Fig. 9b), and volume (Fig. 9c) are greater than the value expected from
20 vertical mixing alone (dashed lines) in the transition layer. This indicates that $E(h)$ is
21 positive for these aerosol properties. These transition layer enhancements are quantified
22 for individual profiles using the difference between the observed value and the value
23 expected from vertical mixing alone. The difference is expressed as a percentage of the
24 observed value and averaged over the transition between normalized altitudes of 1.1 and
25 1.9. The mean transition layer enhancements of aerosol mass, extinction, and volume
26 were +8.6%, +11.3%, and +9.3% respectively. The difference in the enhancements of
27 mass, extinction, and volume may reflect actual changes in the aerosol density and
28 extinction cross-section or could be due to imperfections in the measurements and data
29 aggregation.

30 Altitude-normalized aggregate profiles of aerosol composition are shown in Fig.
31 10. The enhancement of each aerosol component is quantified in the same manner as

1 aerosol mass, extinction, and volume. The observed median is greater than the value
2 expected from vertical mixing alone by +6% for OA mass, +18% for SO₄, +25% for
3 NH₄, and +15% for NO₃. Although enhancement of sulfate is larger than OA as a
4 percentage, the absolute enhancement is a similar magnitude for both SO₄ and OA, ~0.5
5 μg m⁻³.

6 The transition layer enhancements can be further investigated by examining the
7 distribution of enhancements for individual profiles (Fig. 11). For each profile, the
8 enhancement is calculated using the absolute difference between the observed value and
9 that expected from vertical mixing alone. The difference is averaged between normalized
10 altitudes of 1.1 and 1.9. Because the distributions of enhancements range from negative
11 to positive values, the Student's T-test is used to assess if the enhancement distributions
12 are statistically different from zero, or no enhancement. Enhancement distributions with p-
13 values less than 0.05 are considered statistically significant. As expected, Figs. 11a-d
14 shows conserved species that do not have statistically significant enhancements, CH₄,
15 CO₂, H₂O, and black carbon mass. The enhancement distributions of aerosol mass,
16 extinction, and volume (Fig. 11e-g) are all statistically significant. Although both OA
17 and inorganic aerosol components are enhanced in the transition layer, the enhancement
18 distribution of OA is not statistically significant while the enhancement distribution of
19 inorganic components is significant.

20 Secondary aerosol formation in the transition layer is the likely mechanism that
21 would lead to the observed enhancement of aerosol mass, volume, and extinction. The
22 enhancement of aerosol loading is the net result of production and loss in the transition
23 layer; however, profiles of black carbon and total sulfur (see section 4.2) suggest that the
24 aerosol losses are small. Secondary aerosol formation in the transition layer is a
25 combination of aqueous production (both in clouds ~~and~~ and in aerosol water),
26 homogenous oxidation followed by condensation on existing particles, and condensation
27 of semi-volatile species such as NH₄NO₃. The presence of clouds within the transition
28 layer suggests a large role for aqueous production; however, our dataset does not allow us
29 to determine the relative importance of each pathway.

30 Biomass burning, ~~common during the summer in the SEUS,~~ emits aerosol in
31 buoyant plumes that, if large enough, could contribute to the observed enhancement of

1 aerosol loading in the transition layer and would not be consistent with the simple vertical
2 mixing model used here to describe the transition layer concentrations. Biomass burning
3 is common in the SEUS during the fall, winter, and spring-, but is less common during
4 the summer. Zhang et al. [2010] found that biomass burning contributed between 2 and
5 10% to measurements of PM_{2.5} in the summer of 2007 and significantly more in other
6 seasons. Although, biomass burning plumes from agricultural fires were transected on
7 level flight legs during both SENEX and SEAC⁴RS, none of the profiles used in this
8 analysis Profiles during which included fresh biomass burning plumes. were sampled
9 have been excluded from this analysis. However, the possibility remains that the
10 aggregate profiles are contaminated by aged and diluted biomass burning plumes which
11 have not been identified. To address this we considered biomass burning emission factors
12 of black carbon, sulfate, and sulfur dioxide (SO₂, which is oxidized in the atmosphere to
13 sulfate) reported by Akagi et al. [2011]. The emission factors range from 0.20 g/kg to
14 0.91 g/kg for black carbon mass and 0.45 g/kg to 0.87 g/kg for the combination of SO₂
15 and sulfate. Based on these emission factors, we would expect the ratio of the
16 combination of SO₂ and sulfate mass to black carbon mass in biomass burning plumes to
17 range from 0.5 to 4.35. If the observed enhancement of sulfate (~0.5 μg/m³), were due
18 exclusively to biomass burning, we would expect a concomitant enhancement of black
19 carbon (based on the ratio of emission factors for black carbon and sulfate) in the range
20 of 100 to 1000 ng/m³, which is not observed in the profile of black carbon mass (Fig. 8e).
21 Hence, we conclude the enhancement observed in the altitude-normalized aggregate
22 profile is not due to biomass burning.

23

24 **4.2 Sulfur budget**

25 Further evidence for the transition layer enhancement of particulate sulfate comes
26 from the reduction of the concentration of gas-phase SO₂ in the transition layer.
27 Particulate sulfate is produced through gas-phase and aqueous oxidation of SO₂ [*Seinfeld*
28 *and Pandis, 1998*]. We expect that mixing in the transition layer would conserve total
29 sulfur which we define as the sum of particulate sulfate and gas phase SO₂. While
30 particulate sulfate is enhanced in the transition layer as described in Sect. 4.1, there is
31 also a reduction in the mixing ratio of gas phase SO₂ in the transition layer. Figures 12a-c

1 shows altitude-normalized aggregate profiles and values expected from vertical mixing
2 alone for particulate sulfate, gas phase SO₂, and the total sulfur. Particulate sulfate (Fig
3 12a) is enhanced by approximately the same amount as the reduction of SO₂ (Fig. 12b),
4 ~0.1 ppbv in the transition layer. Consequently, the median value of total sulfur agrees
5 well with the value expected from vertical mixing alone.

6 The enhancement distributions for particulate sulfate, SO₂, and total sulfur are
7 shown in Figs. 12 d-f. While the transition layer enhancement of particulate sulfate is
8 significant with a p-value of 3×10^{-5} (Fig. 12d), the reduction of SO₂ in the transition
9 layer (Fig. 12e) is not. The lack of statistical significance in SO₂ reduction is due to
10 positive outliers in the enhancement distribution. The enhancement distribution of total
11 sulfur indicates a small enhancement that is not statistically significant (Fig. 12f). We
12 note that the conservation of sulfate and SO₂ is only apparent when mixing in the
13 transition layer is taken into account. If biomass burning were the source of the transition
14 layer enhancement of particulate sulfate, we expect that total sulfur would be enhanced as
15 well as a similar magnitude to particulate sulfate in the transition layer.

16

17 4.3 Aerosol Optical Depth

18 Aerosol optical depth (AOD) is typically measured remotely from space-based
19 satellites [King *et al.*, 1999] and by ground-based sun photometer networks [Holben *et*
20 *al.*, 2001]. These remote measurements of AOD have been complemented by AOD
21 calculated from aircraft-based in situ measurements of extinction which have the ability
22 to quantify contributions to the AOD from individual layers and aerosol water
23 [Crumeyrolle *et al.*, 2014; Esteve *et al.*, 2012]. Calculated from in situ measurements,
24 AOD is the integral of the ambient aerosol extinction coefficient (σ_{ext}), Eq. 65

25

$$26 \quad AOD = \int_{surface}^{TOA} \sigma_{ext}(z) dz. \quad (65)$$

27

28 where σ_{ext} is a function of altitude z and the integration extends to the top of the
29 atmosphere (TOA). The extinction coefficient in Eq. 65 is at ambient relative humidity,
30 pressure and temperature. Several assumptions are necessary to calculate ambient

1 extinction and subsequently AOD. First, the aircraft profiles of dry extinction, relative
2 humidity, pressure, and temperature must be extrapolated to the surface. [Because](#)
3 [extinction at the surface and aloft in the mixed layer are correlated \(Fig. 4\)](#), the dry
4 extinction is extrapolated as a constant to the surface based on the mean extinction
5 measured in the lowest 200 m of each profile. Relative humidity is extrapolated to the
6 surface using the linear trend in the lowest 200 m of each profile if the trend is positive
7 (RH increases with increasing altitude); otherwise, it is extrapolated as a constant based
8 on the mean RH of the lowest 200 m of each profile. Pressure and temperature are both
9 extrapolated using the linear trend in the lowest 200 m of each profile. The second
10 assumption is that the contributions to AOD from aerosol layers above top of the aircraft
11 profile are negligible. For example, smoke from large forest fires in the western US can
12 be lofted high into the troposphere and transported over the SEUS [Peltier *et al.*, 2007].
13 This contribution to AOD cannot be included if the smoke layer were above the
14 maximum altitude of the profile. In this case the AOD calculated from the in situ profiles
15 is a lower limit. Third, we neglect the contribution to the AOD from supermicroeter
16 particles, which we estimate to be less than 10% of the sub-micrometer AOD based on
17 coarse particle size distribution measurements made during both SENEX and SEAC⁴RS.
18 Fourth, because we have restricted calculated aerosol hygroscopic growth to RH values
19 less than 95%, the AOD calculated here is only a lower limit.

20 In addition to the AOD for each profile in the altitude-normalized aggregate, we
21 have also calculated the contributions to AOD from the mixed layer, the transition layer,
22 aerosol water, and the enhancement of aerosol extinction in the transition layer. The
23 median calculated AOD was 0.14 and the interquartile range (IQR) spanned 0.10 to 0.20
24 (Fig. 13a). An idealized profile of extinction during shallow cumulus convection is used
25 to show the contributions to AOD from the transition layer enhancement of extinction
26 (Fig. 13b), aerosol water (Fig. 13c), the transition layer (Fig. 13d), and the mixed layer
27 (Fig. 13e). The contribution of the transition layer enhancement of ambient extinction
28 (median: 7%, IQR: 4%-10%) is split between the enhancement of dry extinction and the
29 aerosol water associated with the additional aerosol loading. The contribution of aerosol
30 water to the whole profile (median: 33%, IQR: 24%-38%) is sensitive to the aerosol
31 hygroscopicity parameter and ambient RH encountered. The transition layer contribution

1 (median: 45%, IQR: 33%-55%) was slightly smaller than the mixed layer contribution
2 (median: 48%, IQR: 38%-57%). The mixed layer's slightly greater vertical extent and
3 higher average dry extinction favor a larger contribution to AOD; however, the transition
4 layer also provides a substantial contribution to AOD because of the aerosol water
5 associated with the higher mean RH in the transition layer. The contributions to AOD
6 presented in Fig. 13 have substantial overlap (i. e. aerosol water also contributes to mixed
7 and transition layer AOD contributions); hence, the contributions do not add to unity.

8 The altitude-normalized aggregate profiles used in this analysis are drawn from
9 37 vertical profiles; however, they represent only eight afternoons during the summer of
10 2013. For comparison and context, Fig. 14 shows an extended time series of 532 nm
11 AOD (level 2 data) measured by AERONET sun photometers [Holben et al., 2001] at the
12 Centreville SEARCH site and at the Georgia Tech site in Atlanta, Georgia. The Georgia
13 Tech site is in an urban area and is perhaps biased toward larger AOD from urban
14 emissions, while the Centreville site is rural. The sun photometers only report data
15 during cloud-free conditions. Plotted on top of these data from the sun photometers are
16 the AOD from the profiles used in the altitude-normalized aggregate. These data are
17 grouped into the profiles from the SENEX and SEAC⁴RS studies. Aircraft profiles
18 during the SENEX study did not sample AOD greater than 0.3 while the maximum of
19 AOD observed by the sun photometers was greater than 0.4. Profiles during the
20 SEAC⁴RS study, although limited in number, cover a range of AOD similar to the sun
21 photometers. Because the majority of the profiles in the altitude-normalized aggregate
22 are from the SENEX study, the aggregate may be biased toward cleaner conditions. The
23 range of AOD observed during summers of 2011-2013 at the Georgia Tech site indicate
24 that the summer of 2013 is not an outlier with AOD higher or lower than typical
25 summers. This is consistent with the analysis of Kim et al. [2015] who has compared
26 satellite measurements of AOD during the summers 2006-2013.

27 _____ For comparison, Fig 13a (dashed) shows a histogram of 500 nm AOD
28 (measured by an AERONET sun photometer [Holben et al., 2001] at the Centreville
29 SEARCH site) constructed from all available data between 1 May and 30 September
30 2013. The AOD from the sun photometer is higher than the AOD from the profiles in the
31 normalized aggregate, and this difference likely reflects bias in sampling shallow

1 ~~cumulus convection during the in situ profiles compared to more uniform sampling by~~
2 ~~the sun photometer. The in situ profiles presented here are weighted toward relatively~~
3 ~~clean early summer conditions in the presence of shallow cumulus convection, and may~~
4 ~~be biased against late summer biomass burning influence from the western U.S. and~~
5 ~~Canada.~~

6 Several SEUS studies have noted decreases in anthropogenic emissions (sulfur, nitrogen
7 oxides, and volatile organic compounds) in the first decade of the 21st century [Alston *et al.*, 2012; Attwood *et al.*, 2014; Hand *et al.*, 2012; Hand *et al.*, 2013]. Concurrently,
8 particulate sulfate, OA, and AOD have also decreased. Alston *et al.* [2012] have shown
9 that the summertime mean AOD over Georgia reported by the MISR instrument on the
10 Terra spacecraft decreased from ~0.3 in the summer of 2000 to less than 0.2 in the
11 summer of 2009, which is in the range of AOD calculated in this work for the summer
12 2013.
13

14

15 **5. Conclusions**

16 Several preceding studies have observed vertical transport of trace gases and
17 aerosol from the mixed layer into the cloud-influenced transition layer during shallow
18 cumulus convection [Angevine, 2005; Ching and Alkezweeny, 1986; Greenhut, 1986;
19 Langford *et al.*, 2010]. Our observations are consistent with this earlier work. In
20 addition to vertical transport and redistribution of aerosol, we observed a modest
21 enhancement of aerosol loading in the transition layer and conclude that secondary
22 aerosol formation in the transition layer is the likely source of the enhancement.
23 Although we cannot distinguish between condensational and aqueous aerosol formation
24 pathways, the presence of clouds and elevated relative humidity in the transition layer
25 suggests a potential role for aqueous reactions. Using measurements of particulate
26 oxalate as a tracer for aqueous processing, Wonaschuetz *et al.* [2012] and Sorooshian *et al.*
27 [2007] have also observed evidence for secondary aerosol formation in the transition
28 layer during cumulus convection over Texas and near the coast of California.
29 Wonaschuetz *et al.* [2012] show no trends in the OA and particulate sulfate mass
30 fractions with altitude in the mixed and transition layers, which could occur if the
31 production was sufficiently small or if the additional aerosol mass in the transition layer

1 were produced with the same ratio of OA and particulate sulfate that was originally
2 present in the mixed layer. In contrast, our measurements show a distinct difference in
3 composition between the mixed and transition layers and imply a similar magnitude of
4 secondary sulfate and OA production in the transition layer, although the production of
5 OA was not statistically significant.

6 Goldstein et al. [2009] and Ford and Heald [2013] hypothesized a layer of aerosol
7 ~~that is primarily composed of SOA~~, that would be sufficient to explain a significant
8 fraction of the observed summertime enhancement of AOD (2-3 times greater than
9 winter), and that does not contribute to aerosol mass at the surface. The hypothesis is
10 partially supported by the spatial similarity of summertime biogenic emission and
11 summertime AOD over the SEUS. Although, Alston et al. [2012] found that the spatial
12 similarity depended on the spatial resolution AOD of the data used in the analysis, and
13 their analysis of AOD and surface aerosol mass over Georgia did not fully support the
14 hypothesis. Kim et al. [2015] found that the increase of the planetary boundary layer
15 height during the summer could bring the seasonality of the AOD and surface aerosol
16 mass into agreement without the need for an enhanced aerosol layer aloft.

17 Here, we have examined in situ vertical profiles of aerosol and found the dry
18 aerosol to be well mixed in the lowest layer. Above the lowest layer, the aerosol mass
19 and extinction decreased with increasing altitude above that layer (Figs. 3-5). The
20 hygroscopic growth of aerosol at high RH resulted in a layer of enhanced extinction near
21 the top of the mixed layer. The aerosol water accounted for approximately a third of the
22 AOD which would explain a portion of the summertime AOD enhancement. The
23 hypothesized, large enhancement of secondary aerosol aloft was not apparent in these
24 aggregate profiles. However, after normalizing the altitude to the vertical structure and
25 using the CO concentration to quantify the vertical mixing (Figs. 7-10), we were able to
26 resolve a ~~Although we have observed modest an~~ enhancement of aerosol in the transition
27 layer. ~~This layer was~~ is not consistent with the hypothesized layer in magnitude of,
28 and the observed composition was not consistent with the SOA dominated layer
29 hypothesized by Goldstein et al. (2009). We observed enhancements that were less than
30 10% of AOD, and sulfate and OA were enhanced by similar magnitude although the OA
31 enhancement was not statistically significant. The seasonality of the enhancement of

1 surface aerosol mass (less than 1.6 times greater in summer than winter) compared to the
2 AOD enhancement (2-3 times) was the primary evidence for the hypothesized layer.
3 Given the absence of such a layer, our observations suggest that other factors such as
4 meteorology and transport may influence the seasonality of the relationship of AOD to
5 surface aerosol mass and warrant further investigation.

6

7 **Acknowledgements:**

8 We thank the NOAA WP-3D and NASA DC-8 scientists, flight crews and support
9 staff for their outstanding efforts in the field. In particular we would like to thank M. K.
10 Trainer for flight planning during SENEX. Isoprene measurements during SEAC⁴RS
11 were supported by BMVIT / FFG-ALR in the frame of the Austrian Space Application
12 Program (ASAP 8, project 833451). PCJ, DAD, and JLJ measure aerosol mass and
13 composition during SEAC⁴RS and were supported by NASA NNX12AC03G and NSF
14 AGS-1243354. Additionally, the SEARCH aerosol network provided surface
15 measurement used in overflight comparisons, and we thank Brent Holben and Brad
16 Gingrey and their staff for establishing and maintaining the Centreville AERONET sites
17 used in this investigation. This analysis is funded by the NOAA's Health of the
18 Atmosphere Program and Atmospheric Chemistry, Carbon Cycles, and Climate Program
19 and by NASA's Radiation Sciences Program under Award NNH12AT31I.

20

21 **References**

- 22 Akagi, S. K., R. J. Yokelson, C. Wiedinmyer, M. J. Alvarado, J. S. Reid, T. Karl, J. D.
23 Crouse, and P. O. Wennberg (2011), Emission factors for open and domestic
24 biomass burning for use in atmospheric models, *Atmospheric Chemistry and*
25 *Physics*, 11(9), 4039-4072, doi: 10.5194/acp-11-4039-2011.
- 26 Alston, E. J., I. N. Sokolik, and O. V. Kalashnikova (2012), Characterization of
27 atmospheric aerosol in the US Southeast from ground- and space-based
28 measurements over the past decade, *Atmospheric Measurement Techniques*, 5(7),
29 1667-1682, doi: 10.5194/amt-5-1667-2012.
- 30 Angevine, W. M. (2005), An integrated turbulence scheme for boundary layers with
31 shallow cumulus applied to pollutant transport, *J. Appl. Meteorol.*, 44(9), 1436-1452,
32 doi: 10.1175/jam2284.1.
- 33 Attwood, A. R., et al. (2014), Trends in sulfate and organic aerosol mass in the Southeast
34 U.S.: Impact on aerosol optical depth and radiative forcing, *Geophys. Res. Lett.*, 41,
35 7701-7709, doi: 10.1002/2014GL061669.

- 1 Bahreini, R., E. J. Dunlea, B. M. Matthew, C. Simons, K. S. Docherty, P. F. DeCarlo, J.
2 L. Jimenez, C. A. Brock, and A. M. Middlebrook (2008), Design and operation of a
3 pressure-controlled inlet for airborne sampling with an aerodynamic aerosol lens, in
4 *Aerosol Science and Technology*, edited, pp. 465-471.
- 5 Bahreini, R., et al. (2009), Organic aerosol formation in urban and industrial plumes near
6 Houston and Dallas, Texas, *Journal of Geophysical Research-Atmospheres*, 114,
7 doi: 10.1029/2008jd011493.
- 8 Bergstrom, R. W., P. B. Russell, and P. Hignett (2002), Wavelength dependence of the
9 absorption of black carbon particles: Predictions and results from the TARFOX
10 experiment and implications for the aerosol single scattering albedo, *J. Atmos. Sci.*,
11 59(3), 567-577, doi: 10.1175/1520-0469(2002)059<0567:wdotao>2.0.co;2.
- 12 Brock, C. A., et al. (in preparation), Sensitivity of Aerosol Optical Depth to Aerosol and
13 Meteorological Parameters in the Southeastern United States in Summer.
- 14 Cai, Y., D. C. Montague, W. Mooiweer-Bryan, and T. Deshler (2008), Performance
15 characteristics of the ultra high sensitivity aerosol spectrometer for particles between
16 55 and 800 nm: Laboratory and field studies, *Journal of Aerosol Science*, 39(9), 759-
17 769, doi: 10.1016/j.jaerosci.2008.04.007.
- 18 Canagaratna, M. R., et al. (2007), Chemical and microphysical characterization of
19 ambient aerosols with the aerodyne aerosol mass spectrometer, *Mass Spectrometry*
20 *Reviews*, 26(2), 185-222, doi: 10.1002/mas.20115.
- 21 Carlton, A. G., and B. J. Turpin (2013), Particle partitioning potential of organic
22 compounds is highest in the Eastern US and driven by anthropogenic water,
23 *Atmospheric Chemistry and Physics*, 13(20), 10203-10214, doi: 10.5194/acp-13-
24 10203-2013.
- 25 Carlton, A. G., B. J. Turpin, K. E. Altieri, S. P. Seitzinger, R. Mathur, S. J. Roselle, and
26 R. J. Weber (2008), CMAQ Model Performance Enhanced When In-Cloud
27 Secondary Organic Aerosol is Included: Comparisons of Organic Carbon Predictions
28 with Measurements, *Environ. Sci. Technol.*, 42(23), 8798-8802, doi:
29 10.1021/es801192n.
- 30 Ching, J. K. S., and A. J. Alkezweeny (1986), Tracer Study of Vertical Exchange by
31 Cumulus Clouds, *Journal of Climate and Applied Meteorology*, 25(11), 1702-1711,
32 doi: 10.1175/1520-0450(1986)025<1702:tsoveb>2.0.co;2.
- 33 Ching, J. K. S., S. T. Shipley, and E. V. Browell (1988), Evidence for Cloud Venting of
34 Mixed Layer Ozone and Aerosols, *Atmospheric Environment*, 22(2), 225-242, doi:
35 10.1016/0004-6981(88)90030-3.
- 36 Crumeyrolle, S., G. Chen, L. Ziemba, A. Beyersdorf, L. Thornhill, E. Winstead, R. H.
37 Moore, M. A. Shook, C. Hudgins, and B. E. Anderson (2014), Factors that influence
38 surface PM_{2.5} values inferred from satellite observations: perspective gained for the
39 US Baltimore-Washington metropolitan area during DISCOVER-AQ, *Atmospheric*
40 *Chemistry and Physics*, 14(4), 2139-2153, doi: 10.5194/acp-14-2139-2014.
- 41 de Gouw, J. A., and C. Warneke (2007), Measurements of volatile organic compounds in
42 the earths atmosphere using proton-transfer-reaction mass spectrometry, *Mass*
43 *Spectrometry Reviews*, 26(2), 223-257, doi: 10.1002/mas.20119.
- 44 de Gouw, J. A., and J. L. Jimenez (2009), Organic Aerosols in the Earth's Atmosphere,
45 *Environ. Sci. Technol.*, 43(20), 7614-7618, doi: 10.1021/es9006004.

1 Drewnick, F., et al. (2005), A new time-of-flight aerosol mass spectrometer (TOF-AMS)
2 - Instrument description and first field deployment, *Aerosol Science and Technology*,
3 39(7), 637-658, doi: 10.1080/02786820500182040.
4 Dunlea, E. J., et al. (2009), Evolution of Asian aerosols during transpacific transport in
5 INTEX-B, *Atmospheric Chemistry and Physics*, 9(19), 7257-7287.
6 Eatough, D. J., F. M. Caka, and R. J. Farber (1994), The Conversion of SO₂ to Sulfate in
7 the Atmosphere, *Isr. J. Chem.*, 34(3-4), 301-314, doi: 10.1002/ijch.199400034.
8 Edgerton, E. S., B. E. Hartsell, R. D. Saylor, J. J. Jansen, D. A. Hansen, and G. M. Hidy
9 (2005), The Southeastern Aerosol Research and Characterization Study: Part II.
10 Filter-based Measurements of Fine and Coarse Particulate Matter Mass and
11 Composition, *Journal of the Air & Waste Management Association*, 55(10), 1527-
12 1542, doi: 10.1080/10473289.2005.10464744.
13 Edgerton, E. S., B. E. Hartsell, R. D. Saylor, J. J. Jansen, D. A. Hansen, and G. M. Hidy
14 (2006), The Southeastern Aerosol Research and Characterization Study, part 3:
15 Continuous Measurements of Fine Particulate Matter Mass and Composition,
16 *Journal of the Air & Waste Management Association*, 56(9), 1325-1341, doi:
17 10.1080/10473289.2006.10464585.
18 Ervens, B., B. J. Turpin, and R. J. Weber (2011), Secondary organic aerosol formation in
19 cloud droplets and aqueous particles (aqSOA): a review of laboratory, field and
20 model studies, *Atmospheric Chemistry and Physics*, 11(21), 11069-11102, doi:
21 10.5194/acp-11-11069-2011.
22 Esteve, A. R., J. A. Ogren, P. J. Sheridan, E. Andrews, B. N. Holben, and M. P. Utrillas
23 (2012), Sources of discrepancy between aerosol optical depth obtained from
24 AERONET and in-situ aircraft profiles, *Atmospheric Chemistry and Physics*, 12(6),
25 2987-3003, doi: 10.5194/acp-12-2987-2012.
26 Ford, B., and C. L. Heald (2013), Aerosol loading in the Southeastern United States:
27 reconciling surface and satellite observations, *Atmospheric Chemistry and Physics*,
28 13(18), 9269-9283, doi: 10.5194/acp-13-9269-2013.
29 Goldstein, A. H., C. D. Koven, C. L. Heald, and I. Y. Fung (2009), Biogenic carbon and
30 anthropogenic pollutants combine to form a cooling haze over the southeastern
31 United States, *Proceedings of the National Academy of Sciences of the United States*
32 *of America*, 106(22), 8835-8840, doi: 10.1073/pnas.0904128106.
33 Greenhut, G. K. (1986), Transport of Ozone Between Boundary-Layer and Cloud Layer
34 by Cumulus Clouds, *Journal of Geophysical Research-Atmospheres*, 91(D8), 8613-
35 8622, doi: 10.1029/JD091iD08p08613.
36 Hand, J. L., B. A. Schichtel, W. C. Malm, and M. L. Pitchford (2012), Particulate sulfate
37 ion concentration and SO₂ emission trends in the United States from the early 1990s
38 through 2010, *Atmospheric Chemistry and Physics*, 12(21), 10353-10365, doi:
39 10.5194/acp-12-10353-2012.
40 Hand, J. L., B. A. Schichtel, W. C. Malm, and N. H. Frank (2013), Spatial and Temporal
41 Trends in PM_{2.5} Organic and Elemental Carbon across the United States, *Advances*
42 *in Meteorology*, doi: 10.1155/2013/367674.
43 Hansen, D. A., E. S. Edgerton, B. E. Hartsell, J. J. Jansen, N. Kandasamy, G. M. Hidy,
44 and C. L. Blanchard (2003), The Southeastern Aerosol Research and
45 Characterization Study: Part 1-Overview, *Journal of the Air & Waste Management*
46 *Association*, 53(12), 1460-1471, doi: 10.1080/10473289.2003.10466318.

1 He, C., J. Liu, A. G. Carlton, S. Fan, L. W. Horowitz, H. Levy, II, and S. Tao (2013),
2 Evaluation of factors controlling global secondary organic aerosol production from
3 cloud processes, *Atmospheric Chemistry and Physics*, 13(4), 1913-1926, doi:
4 10.5194/acp-13-1913-2013.

5 Hoff, R. M., and S. A. Christopher (2009), Remote Sensing of Particulate Pollution from
6 Space: Have We Reached the Promised Land?, *Journal of the Air & Waste*
7 *Management Association*, 59(6), 645-675, doi: 10.3155/1047-3289.59.6.645.

8 Holben, B. N., et al. (2001), An emerging ground-based aerosol climatology: Aerosol
9 optical depth from AERONET, *Journal of Geophysical Research-Atmospheres*,
10 106(D11), 12067-12097, doi: 10.1029/2001jd900014.

11 Holloway, J. S., R. O. Jakoubek, D. D. Parrish, C. Gerbig, A. Volz-Thomas, S.
12 Schmitgen, A. Fried, B. Wert, B. Henry, and J. R. Drummond (2000), Airborne
13 intercomparison of vacuum ultraviolet fluorescence and tunable diode laser
14 absorption measurements of tropospheric carbon monoxide, *Journal of Geophysical*
15 *Research-Atmospheres*, 105(D19), 24251-24261, doi: 10.1029/2000jd900237.

16 Hudman, R. C., L. T. Murray, D. J. Jacob, D. B. Millet, S. Turquety, S. Wu, D. R. Blake,
17 A. H. Goldstein, J. Holloway, and G. W. Sachse (2008), Biogenic versus
18 anthropogenic sources of CO in the United States, *Geophys. Res. Lett.*, 35(4), doi:
19 10.1029/2007gl032393.

20 Kim, P. S., et al. (2015), Sources, seasonality, and trends of Southeast US aerosol: an
21 integrated analysis of surface, aircraft, and satellite observations with the GEOS-
22 Chem chemical transport model, *ACPD*, (*submitted*).

23 Kim, S., et al. (2007), Measurement of HO₂NO₂ in the free troposphere during the
24 intercontinental chemical transport experiment - North America 2004, *Journal of*
25 *Geophysical Research-Atmospheres*, 112(D12), doi: 10.1029/2006jd007676.

26 Kim, S. W., M. C. Barth, and M. Trainer (2012), Influence of fair-weather cumulus
27 clouds on isoprene chemistry, *Journal of Geophysical Research-Atmospheres*, 117,
28 doi: 10.1029/2011jd017099.

29 King, M. D., Y. J. Kaufman, D. Tanre, and T. Nakajima (1999), Remote sensing of
30 tropospheric aerosols from space: Past, present, and future, *Bulletin of the American*
31 *Meteorological Society*, 80(11), 2229-2259, doi: 10.1175/1520-
32 0477(1999)080<2229:rsotaf>2.0.co;2.

33 Lack, D. A., and J. M. Langridge (2013), On the attribution of black and brown carbon
34 light absorption using the Angstrom exponent, *Atmospheric Chemistry and Physics*,
35 13(20), 10535-10543, doi: 10.5194/acp-13-10535-2013.

36 Langford, A. O., S. C. Tucker, C. J. Senff, R. M. Banta, W. A. Brewer, R. J. Alvarez, R.
37 M. Hardesty, B. M. Lerner, and E. J. Williams (2010), Convective venting and
38 surface ozone in Houston during TexAQS 2006, *Journal of Geophysical Research-*
39 *Atmospheres*, 115, doi: 10.1029/2009jd013301.

40 Langridge, J. M., M. S. Richardson, D. Lack, D. Law, and D. M. Murphy (2011), Aircraft
41 Instrument for Comprehensive Characterization of Aerosol Optical Properties, Part I:
42 Wavelength-Dependent Optical Extinction and Its Relative Humidity Dependence
43 Measured Using Cavity Ringdown Spectroscopy, *Aerosol Science and Technology*,
44 45(11), 1305-1318, doi: 10.1080/02786826.2011.592745.

1 Luria, M., and H. Sievering (1991), Heterogeneous and Homogeneous Oxidation of SO₂
2 in the Marine Atmosphere, *Atmospheric Environment Part a-General Topics*, 25(8),
3 1489-1496, doi: 10.1016/0960-1686(91)90008-u.

4 Massoli, P., T. S. Bates, P. K. Quinn, D. A. Lack, T. Baynard, B. M. Lerner, S. C.
5 Tucker, J. Brioude, A. Stohl, and E. J. Williams (2009), Aerosol optical and
6 hygroscopic properties during TexAQS-GoMACCS 2006 and their impact on
7 aerosol direct radiative forcing, *Journal of Geophysical Research-Atmospheres*, 114,
8 doi: 10.1029/2008jd011604.

9 McKeen, S., et al. (2007), Evaluation of several PM2.5 forecast models using data
10 collected during the ICARTT/NEAQS 2004 field study, *Journal of Geophysical*
11 *Research-Atmospheres*, 112(D10), doi: 10.1029/2006jd007608.

12 McNaughton, C. S., et al. (2007), Results from the DC-8 Inlet Characterization
13 Experiment (DICE): Airborne versus surface sampling of mineral dust and sea salt
14 aerosols, *Aerosol Science and Technology*, 41(2), 136-159, doi:
15 10.1080/02786820601118406.

16 Middlebrook, A. M., R. Bahreini, J. L. Jimenez, and M. R. Canagaratna (2012),
17 Evaluation of Composition-Dependent Collection Efficiencies for the Aerodyne
18 Aerosol Mass Spectrometer using Field Data, *Aerosol Science and Technology*,
19 46(3), 258-271, doi: 10.1080/02786826.2011.620041.

20 Peischl, J., et al. (2012), Airborne observations of methane emissions from rice
21 cultivation in the Sacramento Valley of California, *Journal of Geophysical*
22 *Research-Atmospheres*, 117, doi: 10.1029/2012jd017994.

23 Peltier, R. E., A. P. Sullivan, R. J. Weber, C. A. Brock, A. G. Wollny, J. S. Holloway, J.
24 A. de Gouw, and C. Warneke (2007), Fine aerosol bulk composition measured on
25 WP-3D research aircraft in vicinity of the Northeastern United States - results from
26 NEAQS, *Atmospheric Chemistry and Physics*, 7(12), 3231-3247, doi: 10.5194/acp-
27 7-3231-2007.

28 Petters, M. D., and S. M. Kreidenweis (2007), A single parameter representation of
29 hygroscopic growth and cloud condensation nucleus activity, *Atmospheric*
30 *Chemistry and Physics*, 7(8), 1961-1971.

31 Quinn, P. K., et al. (2005), Impact of particulate organic matter on the relative humidity
32 dependence of light scattering: A simplified parameterization, *Geophys. Res. Lett.*,
33 32(22), doi: 10.1029/2005gl024322.

34 Ryerson, T. B., et al. (1998), Emissions lifetimes and ozone formation in power plant
35 plumes, *Journal of Geophysical Research-Atmospheres*, 103(D17), 22569-22583,
36 doi: 10.1029/98jd01620.

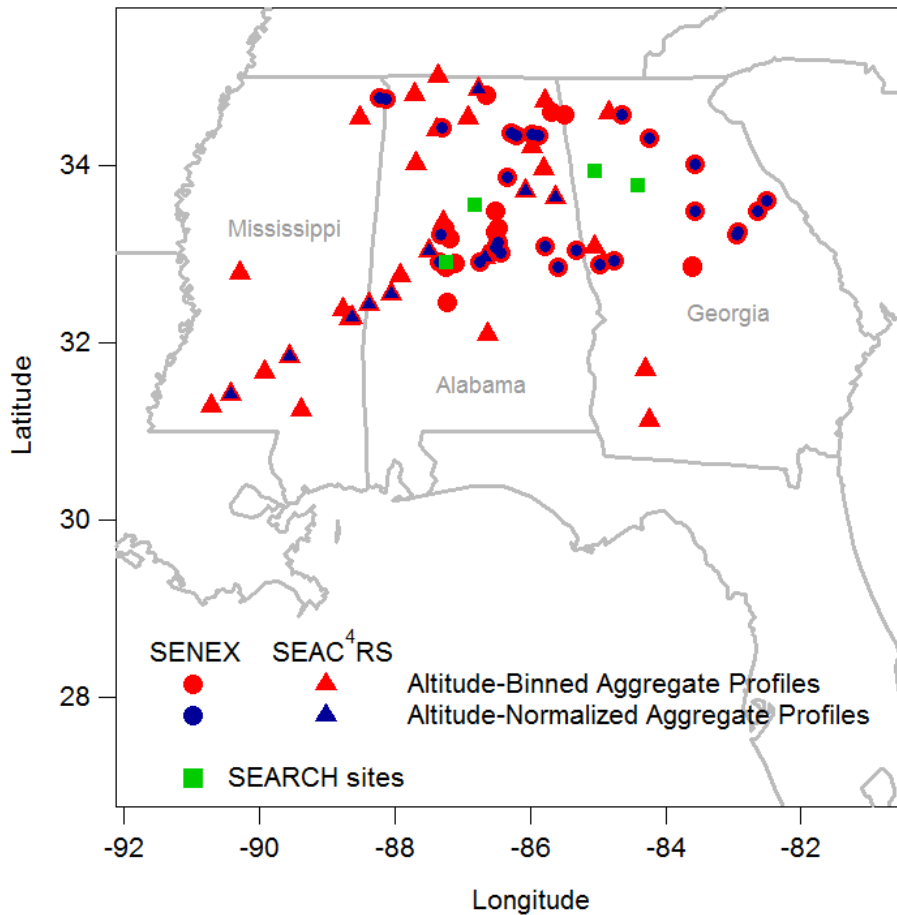
37 Sachse, G. W., G. F. Hill, L. O. Wade, and M. G. Perry (1987), Fast Response, High
38 Precision Carbon Monoxide Sensor Using a Tunable Diode-Laser Absorption
39 Technique, *Journal of Geophysical Research-Atmospheres*, 92(D2), 2071-2081, doi:
40 10.1029/JD092iD02p02071.

41 Santarpia, J. L., R. J. Li, and D. R. Collins (2004), Direct measurement of the hydration
42 state of ambient aerosol populations, *Journal of Geophysical Research-Atmospheres*,
43 109(D18), doi: 10.1029/2004jd004653.

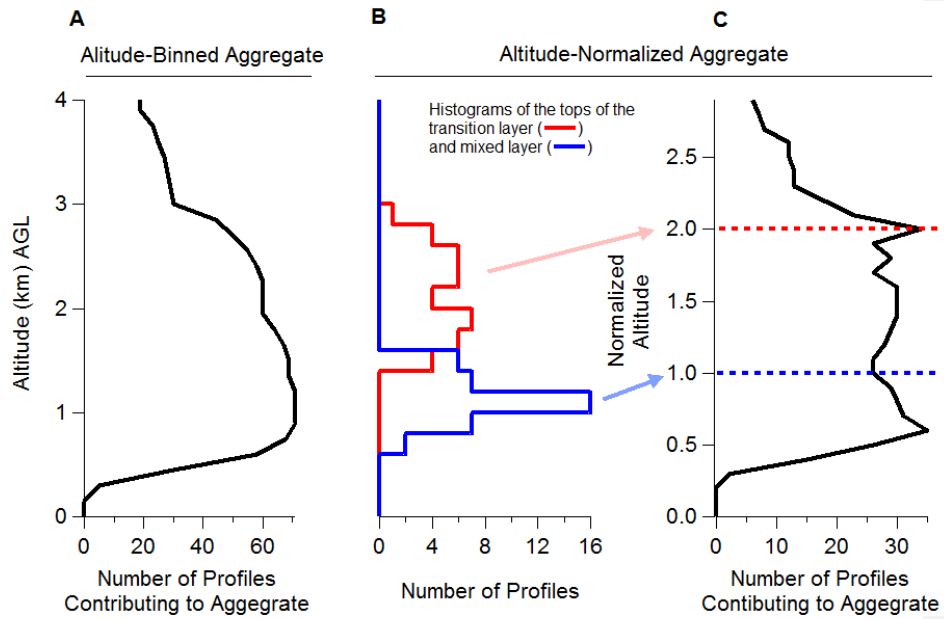
44 Schwarz, J. P., et al. (2008), Measurement of the mixing state, mass, and optical size of
45 individual black carbon particles in urban and biomass burning emissions, *Geophys.*
46 *Res. Lett.*, 35(13), doi: 10.1029/2008gl033968.

- 1 Seinfeld, J. H., and S. N. Pandis (1998), *Atmospheric Chemistry and Physics*, John Wiley
2 & Sons, New York.
- 3 Siebesma, A. P. (1998), Shallow Cumulus Convection, in *Buoyant Convection in*
4 *Geophysical Flows*, edited by E. J. Plate, E. E. Fedorovich, D. X. Viegas and J. C.
5 Wyngaard, pp. 441-486, Kluwer Academic Publishers, Dordrecht.
- 6 Sorooshian, A., M.-L. Lu, F. J. Brechtel, H. Jonsson, G. Feingold, R. C. Flagan, and J. H.
7 Seinfeld (2007), On the source of organic acid aerosol layers above clouds, *Environ.*
8 *Sci. Technol.*, *41*(13), 4647-4654, doi: 10.1021/es0630442.
- 9 Sorooshian, A., et al. (2006), Oxalic acid in clear and cloudy atmospheres: Analysis of
10 data from International Consortium for Atmospheric Research on Transport and
11 Transformation 2004, *Journal of Geophysical Research-Atmospheres*, *111*(D23),
12 doi: 10.1029/2005jd006880.
- 13 Vay, S. A., et al. (2011), Patterns of CO₂ and radiocarbon across high northern latitudes
14 during International Polar Year 2008, *Journal of Geophysical Research-*
15 *Atmospheres*, *116*, doi: 10.1029/2011jd015643.
- 16 Warren, S. G., R. M. Eastman, and C. J. Hahn (2007), A survey of changes in cloud
17 cover and cloud types over land from surface observations, 1971-96, *Journal of*
18 *Climate*, *20*(4), 717-738, doi: 10.1175/jcli4031.1.
- 19 Weber, R. J., et al. (2007), A study of secondary organic aerosol formation in the
20 anthropogenic-influenced southeastern United States, *Journal of Geophysical*
21 *Research-Atmospheres*, *112*(D13), doi: 10.1029/2007jd008408.
- 22 Wilson, J. C., B. G. Lafleur, H. Hilbert, W. R. Seebaugh, J. Fox, D. W. Gesler, C. A.
23 Brock, B. J. Huebert, and J. Mullen (2004), Function and performance of a low
24 turbulence inlet for sampling supermicron particles from aircraft platforms, *Aerosol*
25 *Science and Technology*, *38*(8), 790-802, doi: 10.1080/027868290500841.
- 26 Wonaschuetz, A., A. Sorooshian, B. Ervens, P. Y. Chuang, G. Feingold, S. M. Murphy, J.
27 de Gouw, C. Warneke, and H. H. Jonsson (2012), Aerosol and gas re-distribution by
28 shallow cumulus clouds: An investigation using airborne measurements, *Journal of*
29 *Geophysical Research-Atmospheres*, *117*, doi: 10.1029/2012jd018089.
- 30 Zhang, X., A. Hecobian, M. Zheng, N. H. Frank, and R. J. Weber (2010), Biomass
31 burning impact on PM_{2.5} over the southeastern US during 2007: integrating
32 chemically speciated FRM filter measurements, MODIS fire counts and PMF
33 analysis, *Atmospheric Chemistry and Physics*, *10*(14), 6839-6853, doi: 10.5194/acp-
34 10-6839-2010.

35

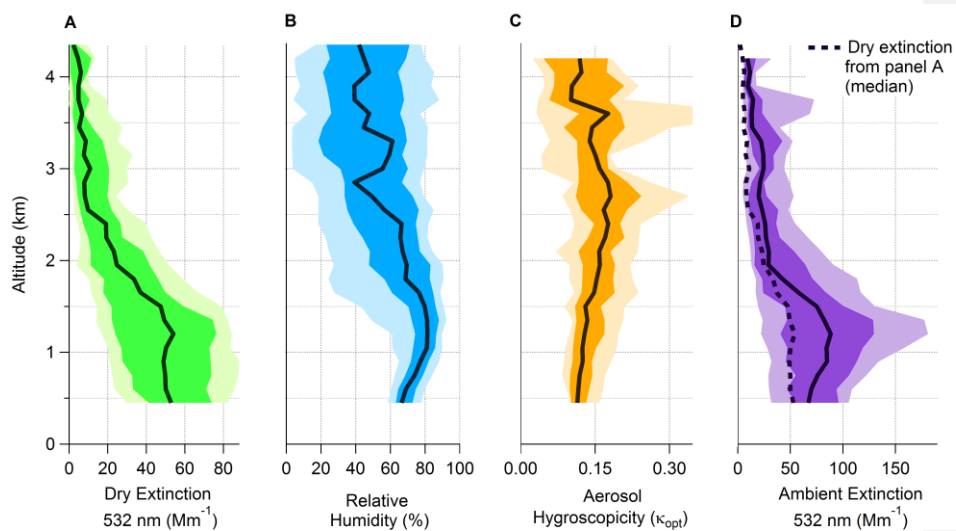


1
2 **Figure 1:** The locations of the vertical profiles from the SENEX (circles) and SEAC⁴RS
3 (triangles) and SEARCH monitoring sites (green squares). The markers (both red and
4 blue) are the locations of afternoon profiles used to construct the altitude-binned
5 aggregate profile that includes 74 profiles: 41 from SENEX and 33 from SEAC⁴RS. The
6 blue markers show the location of the profiles used to construct the altitude-normalized
7 aggregate profile that includes 37 profiles: 27 from SENEX and 10 from SEAC⁴RS.
8



1 **Figure 2:** (A) The number of profiles that contribute to the altitude-binned aggregate,
 2 (B) histograms of the altitude of the tops of the transition and mixed layers, and (C) the
 3 number of profiles that contribute to the altitude-normalized aggregate.
 4
 5

1



2

3

4

5

6

7

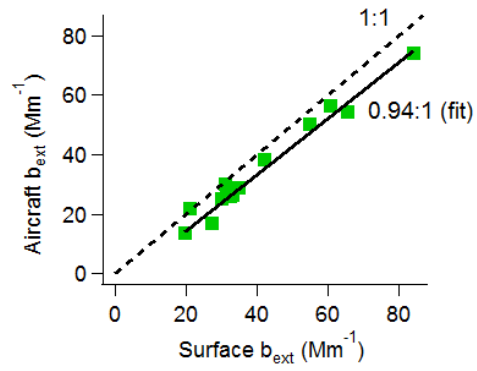
8

9

10

Figure 3: Altitude-binned aggregate profiles of (A) the 532 nm dry aerosol extinction, (B) relative humidity (calculated from dew point measurements), (C) aerosol hygroscopicity (humidified extinction measurements fit to Eq. 1), and (D) the calculated ambient extinction (Eq. 1). The shaded regions show the interdecile range (light) and the interquartile range (medium), and the solid lines are the median (dark). The dashed line in panel D shows the median dry extinction for comparison.

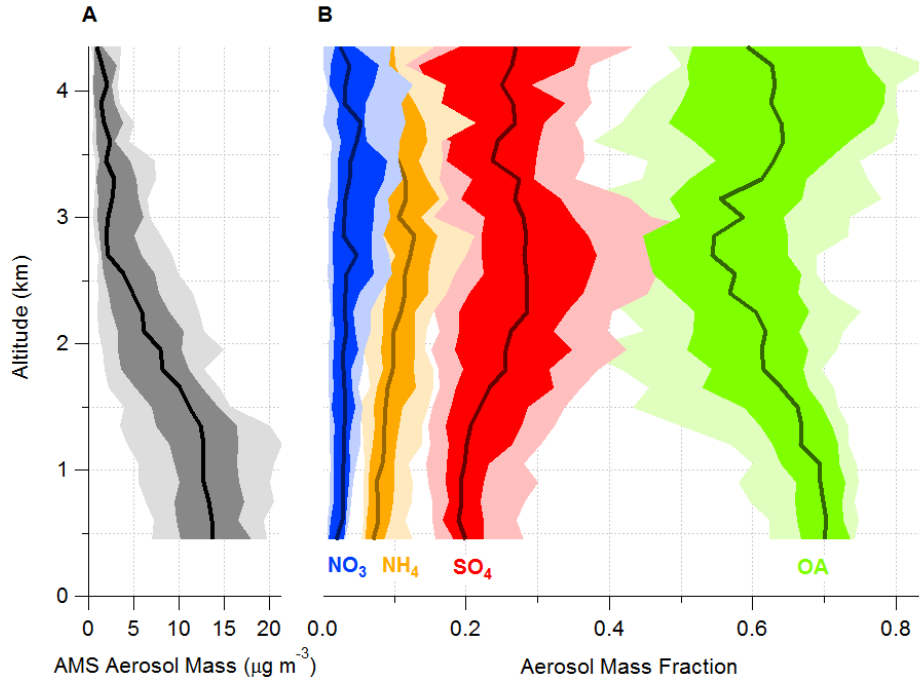
1
2



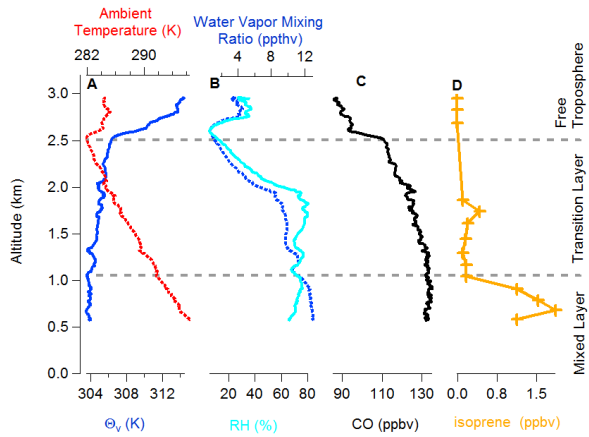
3
4
5
6
7
8

Figure 4: Comparison of airborne and surface measurements of the dry aerosol extinction coefficient. The airborne measurements are aboard the NOAA WP-3 aircraft. The surface measurements are from the SEARCH monitoring sites.

1
2



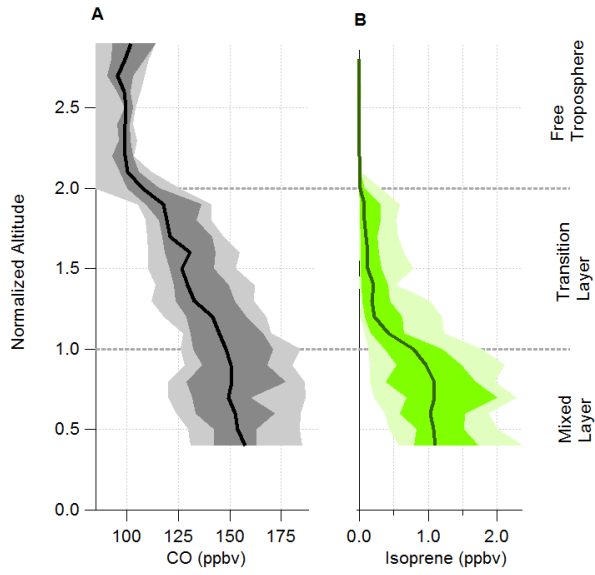
3
4 **Figure 5:** Aggregate profiles of (A) the aerosol mass and (B) the mass fractions of
5 nitrate, ammonium, sulfate, and OA. The shaded regions show the interdecile range
6 (light) and the interquartile range (medium), and the solid lines are the median (dark).
7
8



9

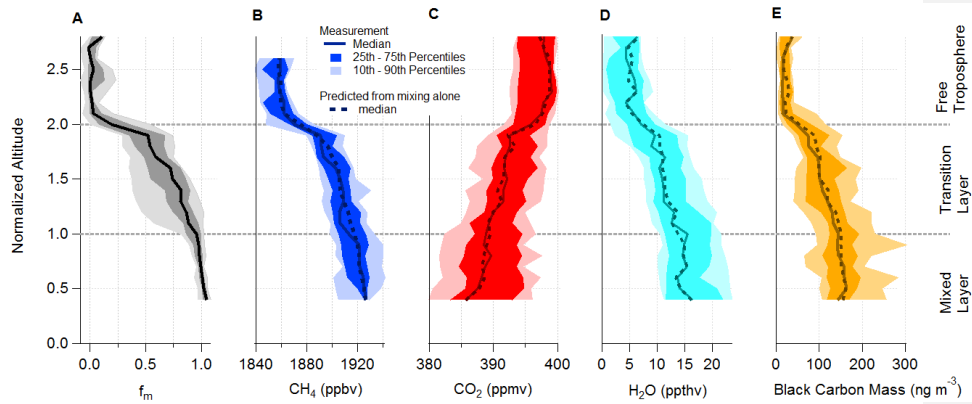
1 **Figure 6:** An example profile collected over central Georgia in the afternoon of 16 June
2 showing (A) the temperature and virtual potential temperature, (B) the relative humidity
3 and the water vapor mixing ratio, (C) the mixing ratio of CO that has a long lifetime, and
4 (D) the mixing ratio of isoprene that has a short lifetime.
5
6

1
2



3
4
5
6
7
8

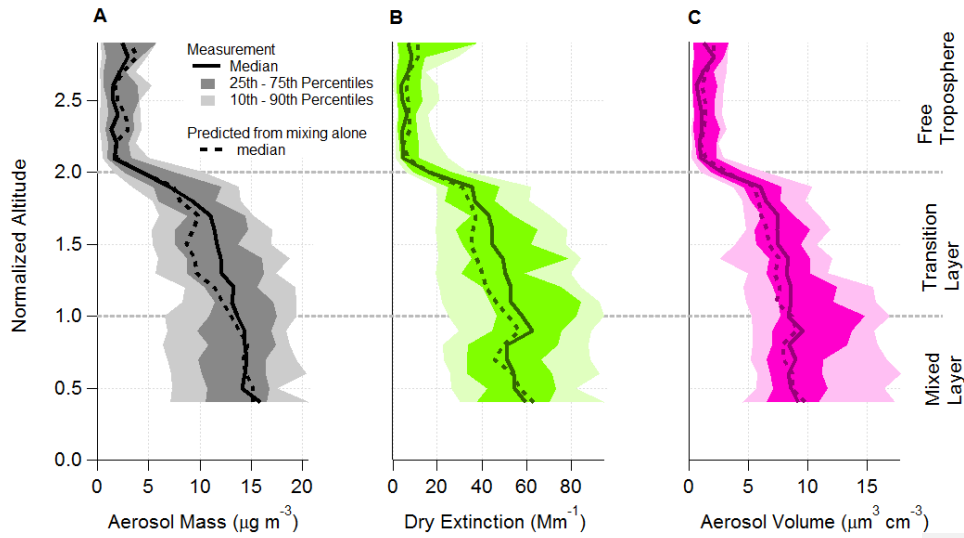
Figure 7: Altitude-normalized aggregate profiles of (A) CO, and (B) isoprene mixing ratios. The shaded regions show the interdecile range (light) and the interquartile range (medium), and the solid lines are the median (dark).



1 **Figure 8:** Altitude-normalized aggregate profile of (A) fraction of mixed layer air (Eq.
 2 4), (B) CH₄, (C), CO₂, (D) H₂O, and (E) black carbon aerosol mass. The dashed line
 3 shows the concentrations expected from vertical mixing alone (Eq. 3). The shaded
 4 regions show the interdecile range (light) and the interquartile range (medium), and the
 5 solid lines are the median (dark). These trace gases and black carbon aerosol mass
 6 are not expected to be enhanced or reduced in the transition layer. The agreement between
 7 the observations and the concentration expected from vertical mixing alone demonstrates
 8 that CO can be used to quantify the fraction air from the mixed layer.
 9

10
 11
 12

1



2

3

4

5

6

7

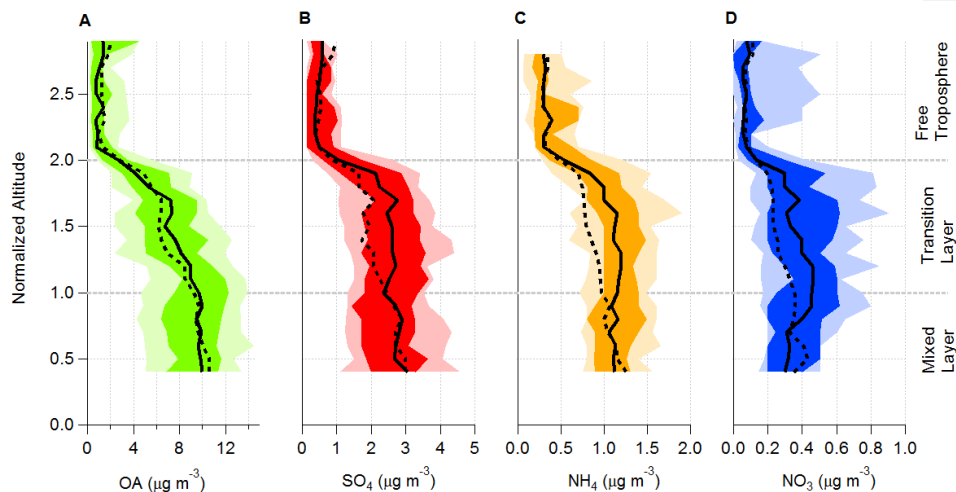
8

9

10

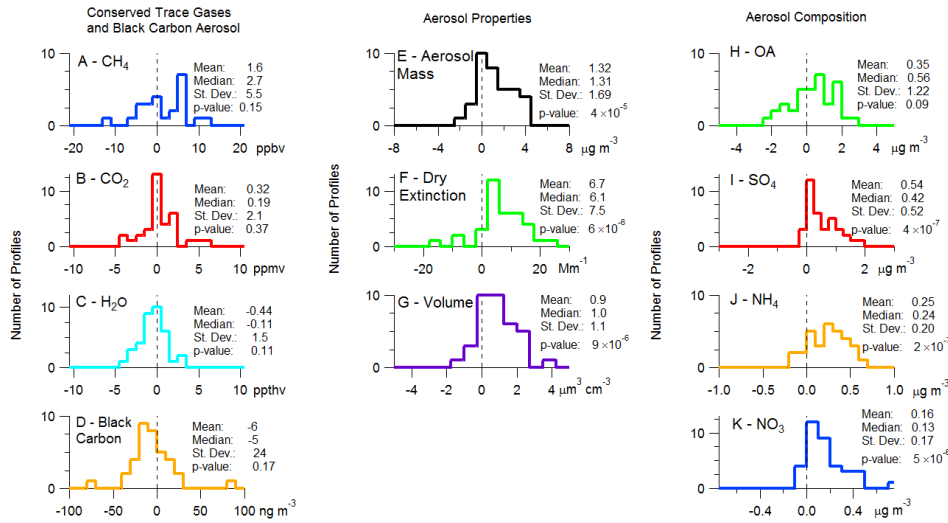
11

Figure 9: Altitude-normalized aggregate profiles of aerosol mass (A), extinction (B), and volume (C). The aerosol volume was calculated from measured particle size distributions. The shaded regions show the interdecile range (light) and the interquartile range (medium), and the solid lines are the median (dark). The dashed line shows the median value expected from mixing alone (Eq. 3). The difference between the observed median value and the median value expected from mixing alone indicates an enhancement of aerosol in the transition layer.

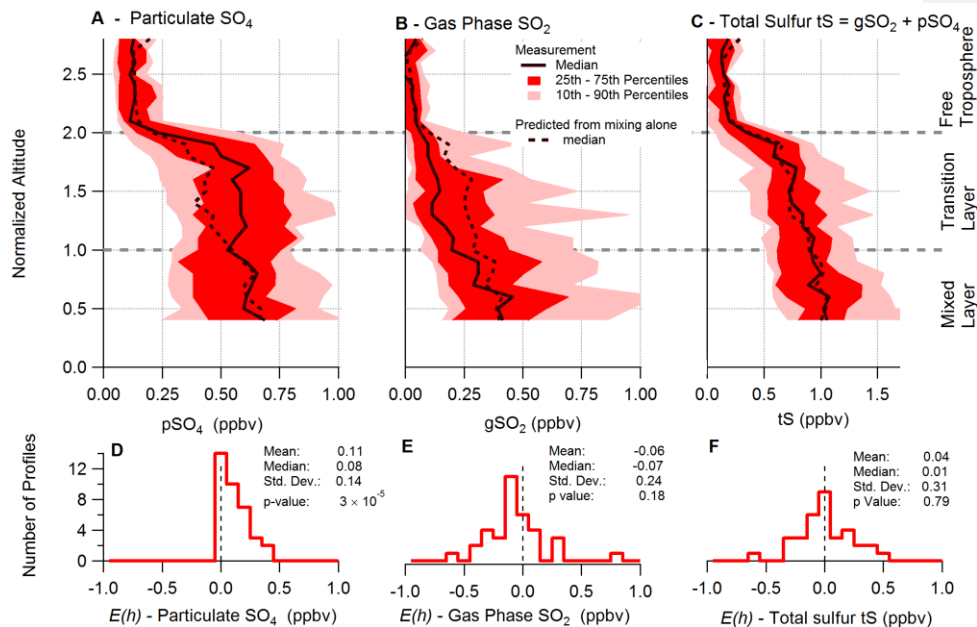


1 **Figure 10:** Altitude-normalized profiles of the aerosol composition: (A) OA, (B) SO_4 ,
 2 (C) NH_4 , and (D) NO_3 . The shaded regions show the interdecile range (light) and the
 3 interquartile range (medium), and the solid lines are the median (dark). The dashed line
 4 shows the median expected concentration from vertical mixing alone (Eq. 3).
 5
 6
 7

1
2

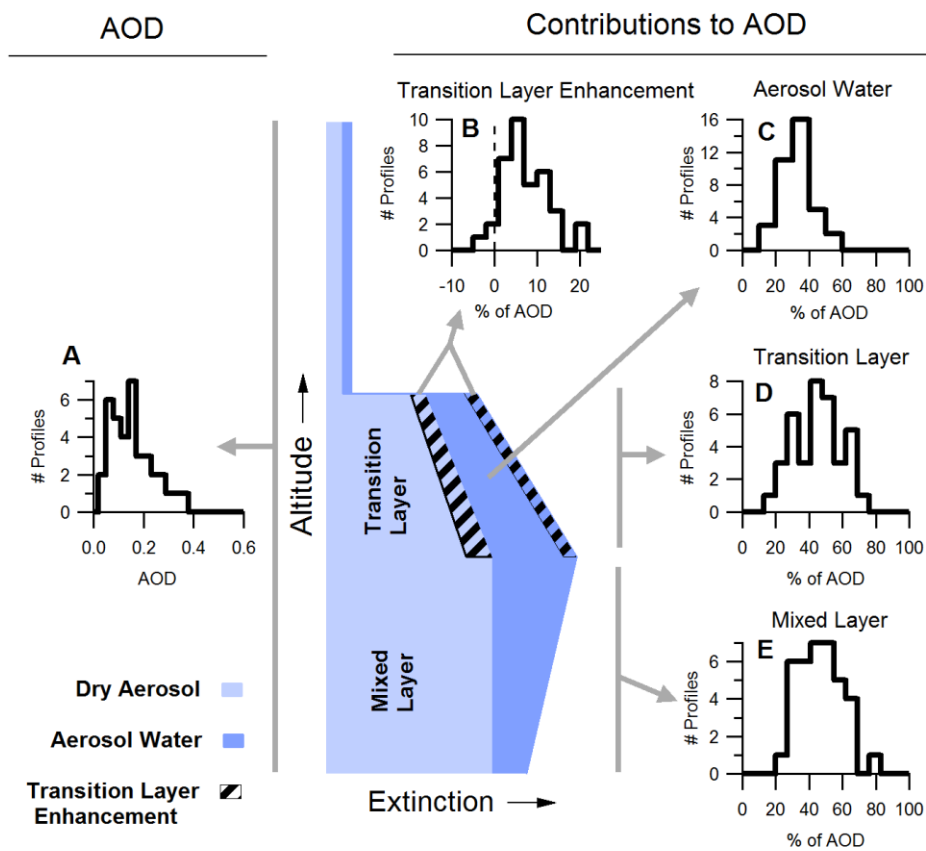


3
4 **Figure 11:** Histograms of the transition layer enhancement ($E(h)$ – see Eq. 4) for several
5 trace gases and aerosol properties. The first column shows conserved species and black
6 carbon: (A) CH₄, (B) CO₂, (C) H₂O, and (D) black carbon mass. The second column
7 shows the aerosol extensive properties: (E) aerosol mass, (F) dry extinction, and (G)
8 aerosol volume. The third column shows the aerosol composition: (H) OA, (I) SO₄, (J)
9 NH₄, and (K) NO₃. The Student's T-test and resulting p-value (noted in each histogram)
10 were used to test if the mean of each distribution was statistically different from zero.

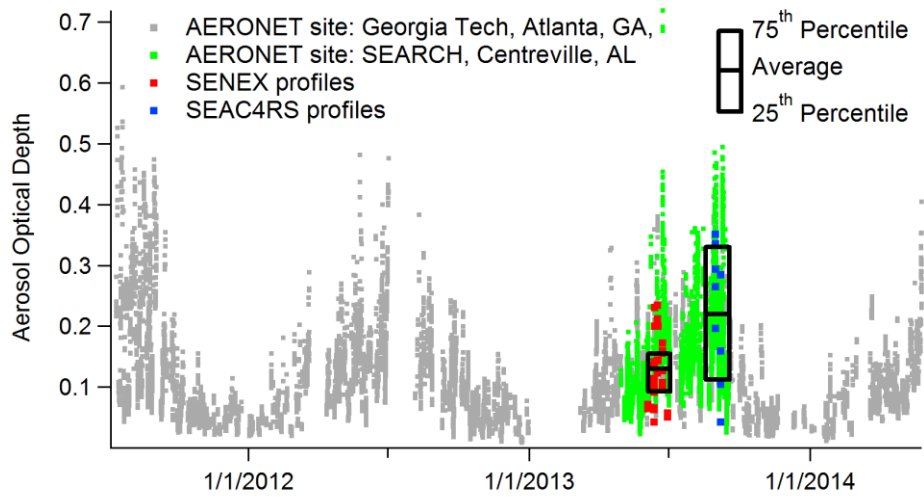


1
2
3
4
5
6
7
8

Figure 12: Altitude-normalized profiles of (A) particulate sulfate, (B) gas phase SO₂, and (C) total sulfur tS. The shaded regions show the interdecile range (light) and the interquartile range (medium), and the solid lines are the median (dark). The dashed line shows the median value expected from mixing alone. Histograms of the transition layer enhancement ($E(h)$) and the results of the T-test for (E) particulate sulfate, (F) SO₂, and (G) total sulfur are shown.



1
 2 **Figure 13:** The AOD contributions of dry aerosol, aerosol water, and enhanced
 3 extinction in the transition layer are illustrated in an idealized profile. [The idealized](#)
 4 [profile of extinction \(blue\) at the center of the figure shows the vertical location of each](#)
 5 [contribution to AOD. The light blue area represents the extinction of dry aerosol, and the](#)
 6 [darker blue area shows the enhancement to aerosol water. The subpanels show \(A\)](#)
 7 [histograms of AOD calculated from individual profiles \(solid\) and AOD measured with a](#)
 8 [sun photometer \(dashed\) at the Centreville SEARCH site, and the contributions to AOD](#)
 9 [from the \(B\) transition layer enhancement of extinction, \(C\) aerosol water, \(D\) the](#)
 10 [transition layer, and \(E\) the mixed layer. The calculated AOD assumes no contribution](#)
 11 [from aerosol above the top of the profile and extrapolates the dry extinction and RH to](#)
 12 [the surface.](#)
 13
 14



1
 2 **Figure 14:** The AOD measured by AERONET sun photometers in Atlanta, GA (gray)
 3 and Centreville, AL (green) and the AOD from the SENEX (red) and SEAC⁴RS (blue)
 4 profiles included in the altitude-normalized aggregate are shown. The black boxes show
 5 the average, 25th, and 75th percentiles of AOD from both the SENEX and SEAC⁴RS
 6 profiles.
 7